

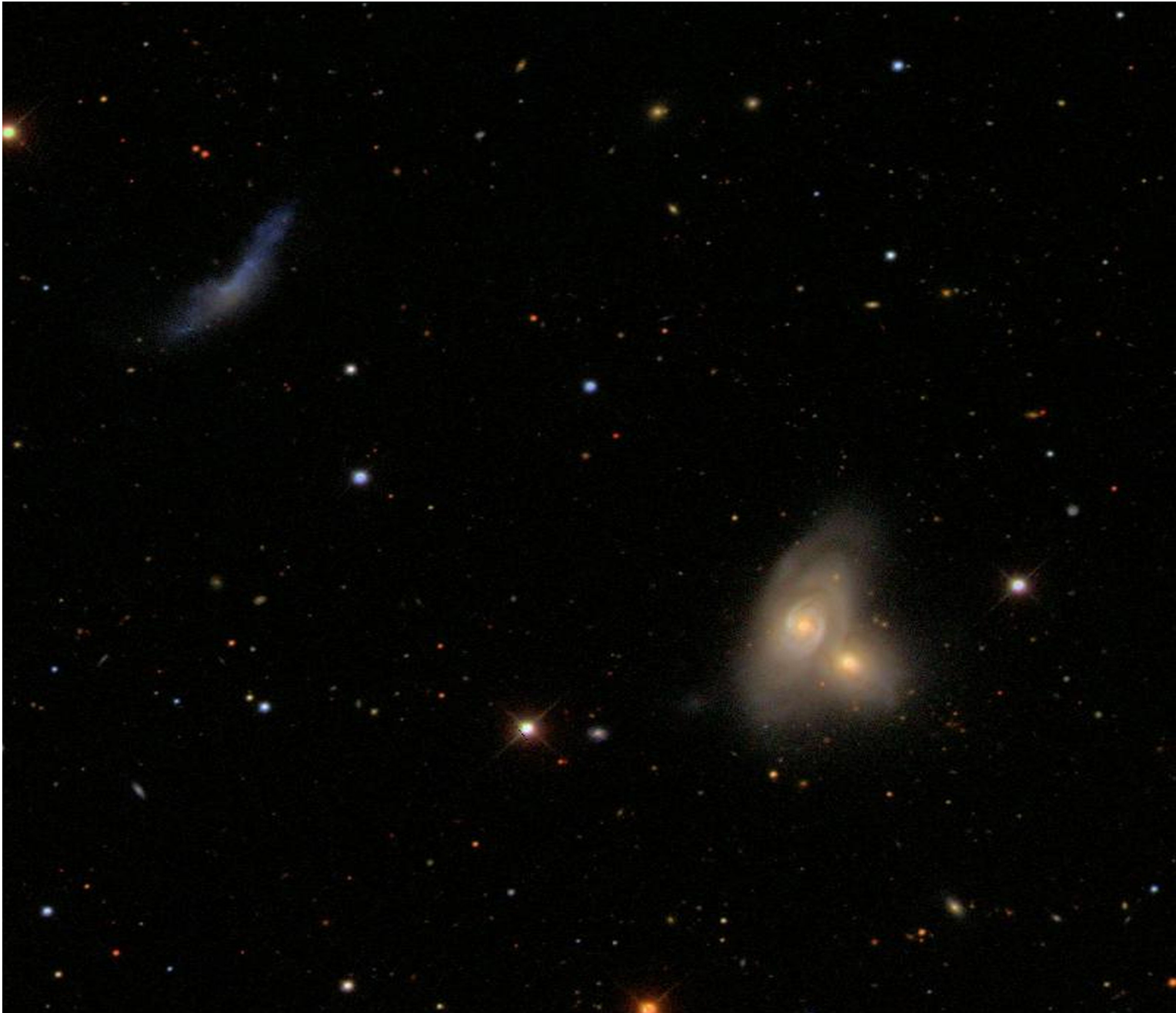
On the composite nature of the galaxy NGC 5929

Georgi Petrov¹ & Michelle Dennefeld²

- 1) Institute of astronomy and National astronomical observatory, Sofia, Bulgaria**
- 2) Institut d'Astrophysique de Paris 98bis Bd Arago FR 75014, Paris, France.**

VIII Serbian-Bulgarian astronomical conference

08-12 MAY, 2012, LESKOVAC, SERBIA

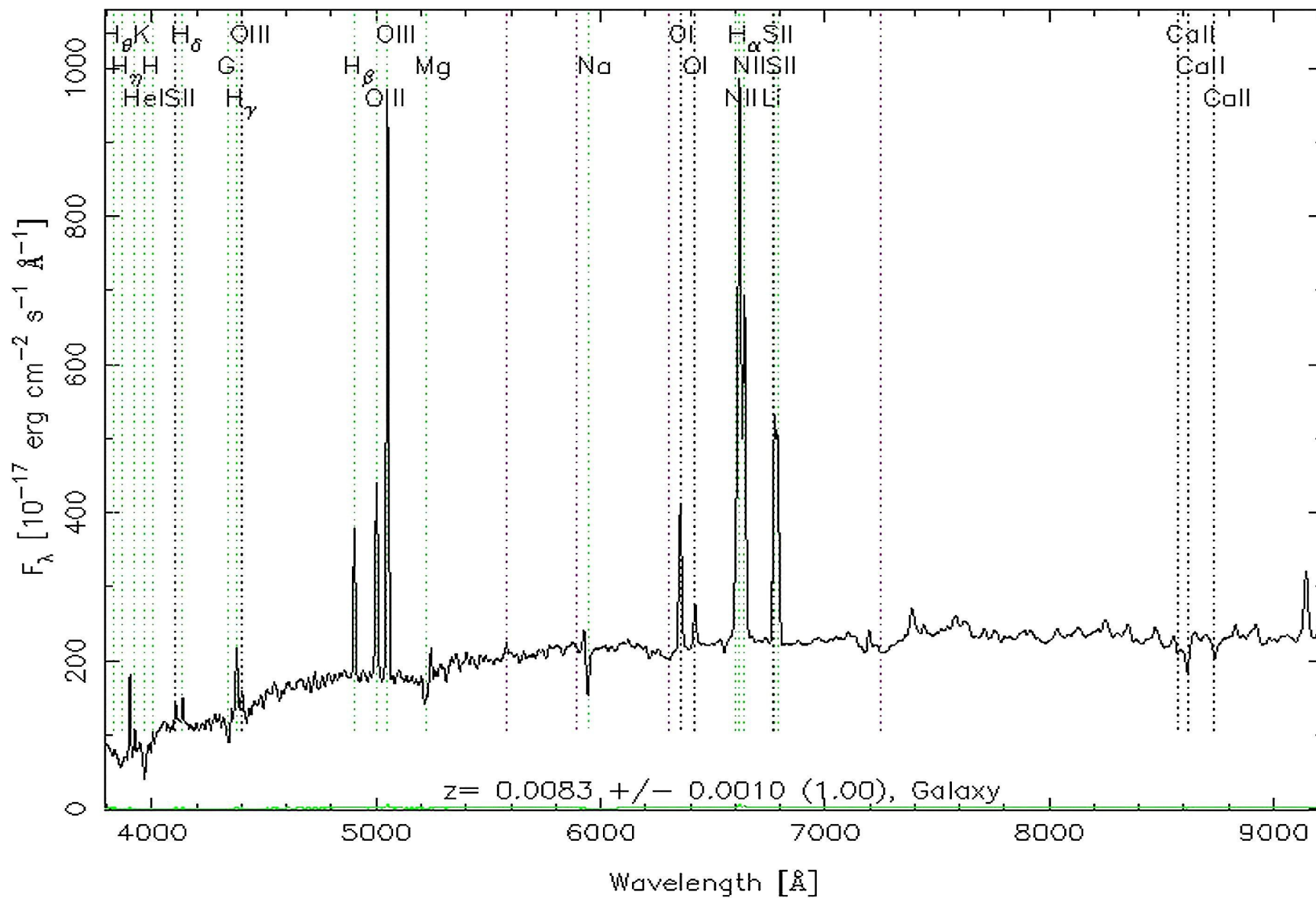


CROSS-IDENTIFICATIONS for NGC 5929 (Back to INDEX)				No.	Frequency Targeted	km/s +/- unc	z +/- unc	Reference Code
Object Names	Type	Object Names	Type					
NGC 5929	G	USGC U703 NED04	G	0		2492 8	0.008312 0.000027	1997A&A...328..493F
UGC 09851	G	HOLM 710B	G	1	Optical features	2504 5	0.008351 0.000016	2005SDSS4.C...0000
ARP 090 NED01	G	NPM1G +41.0399	G	2	21-cm HI line	2561 10	0.008543 0.000033	1991RC3.9.C...0000d
VV 823 NED01	G	PGC 055076	G	3	Optical	2502 14	0.008346 0.000047	1992CORV.C...0000F
I Zw 112 NED01	G	UZC J152606.1+414013	G	4	Optical	2506 22	0.008359 0.000073	2000UZC...C.....0F
CGCG 222-007 NED01	G	FIRST J152606.1+414014	RadioS	5	Optical lines	2514 24	0.008386 0.000080	1991RC3.9.C...0000d
CGCG 1524.3+4151 NED01	G	IRXP J152607.0+414016	XrayS	6	Optical	2436 29	0.008126 0.000097	1992CORV.C...0000F
MCG +07-32-006	G	[SP82] 45	G	7	Optical	2527 50	0.008429 0.000167	1992CORV.C...0000F
SDSS J152606.15+414014.3	G	LGG 399:[G93] 004	G	8	Optical features	2488 296	0.008298 0.000989	2005SDSS4.C...0000
SDSS J152606.16+414014.4	G	[M98j] 242 NED01	G	9	Optical	2504	0.008352	1992CORV.C...0000F
CG 0710	G	[VCV2001] J152606.1+414015	G	10	Optical	2522	0.008412	1992CORV.C...0000F
KPG 466 NED01	G	[RRP2006] 37	G	11	Optical	2525	0.008422	1992CORV.C...0000F
KPG 466A	G	[VCV2006] J152606.1+414015	G	12	Optical	2538	0.008466	1992CORV.C...0000F
				13	Optical	2551	0.008509	1992CORV.C...0000F

Reference(s) for object NGC 5929 : 271 references found in NED (from 1898 to 2011).

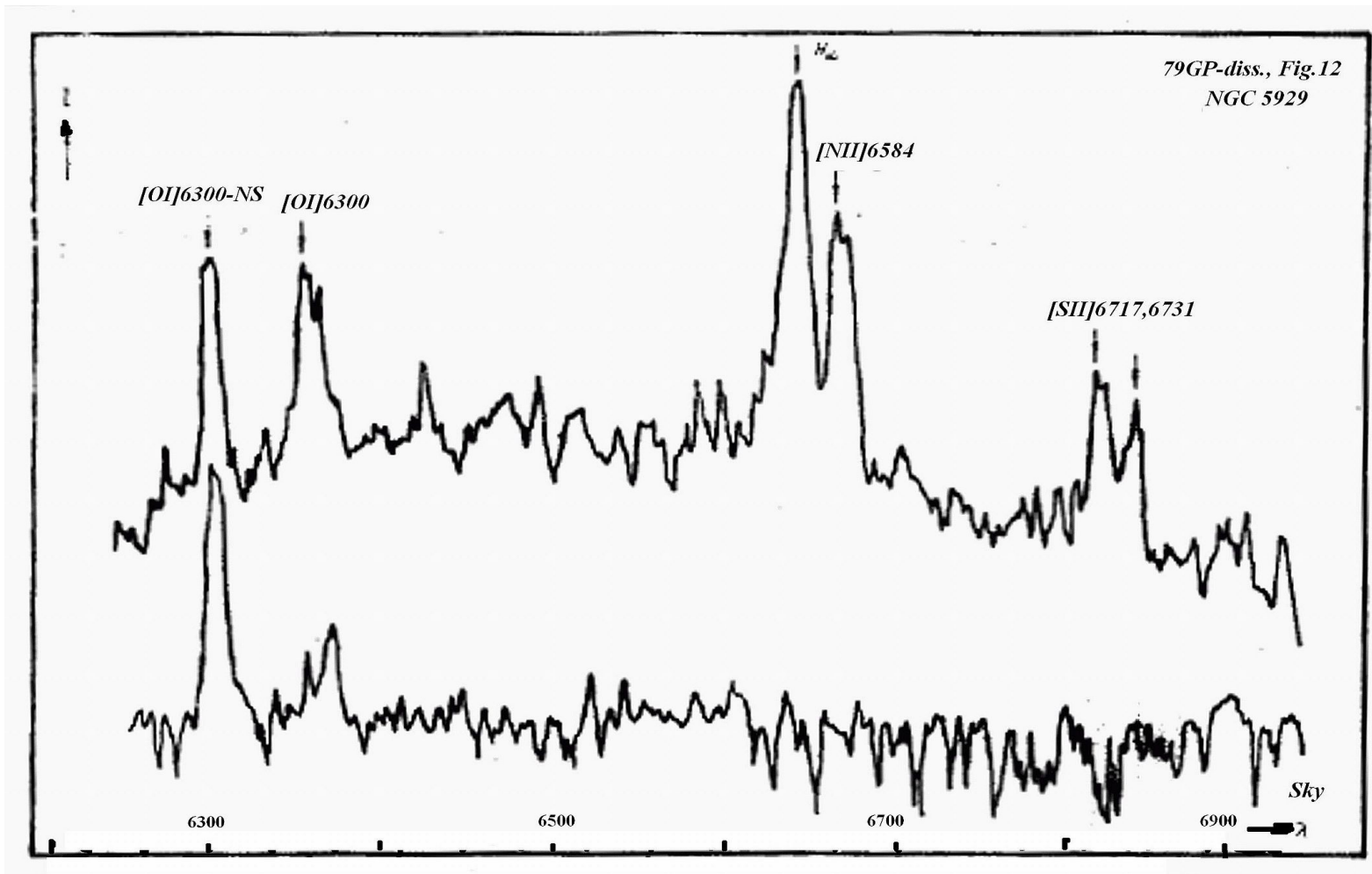
1. [2011ApJ...730..121W](#) WU, YU-ZHONG; Z... THE DIFFERENT NATURE OF SEYFERT 2 GALAXIES WITH AND WITHOUT HIDDEN...
2. [2010ApJS...187..172G](#) GALLIMORE, J. F... INFRARED SPECTRAL ENERGY DISTRIBUTIONS OF SEYFERT GALAXIES: SPITZER...
3. [2010ApJ...725.2270P](#) PEREIRA-SANTAEL... THE MID-INFRARED HIGH-IONIZATION LINES FROM ACTIVE GALACTIC NUCLEI...
4. [2010ApJ...720..786L](#) LAMASSA, STEPHA... INDICATORS OF INTRINSIC ACTIVE GALACTIC NUCLEUS LUMINOSITY: A MULTI-...

N5929-SDSS RA=231.52566, DEC=41.67066, MJD=53149, Plate=1679, Fiber=350



1979, Petrov, "Physical conditions in the nuclei of emission-line galaxies".

...spectrograms obtained with the 125-cm reflector of the Crimean station, Shternberg Astronomical Institute. *NGC 5929 IS NOT a SyG and double_pick emission is not mentioned. First time double pick emission was shown in G. Petrov's PhD thesis – fig.12.*



1980, Golev, V. K.; Yankulova, I. M.; Petrov, G. T.

“The nucleus of the galaxy NGC 5929 - Preliminary spectrophotometry”.

Spectra of the nucleus of the galaxy NGC 5929 obtained with the 1.25-m and 6-m telescopes show emission lines with separate components in the wings. In the blue and red wings of each line one can see components shifted 5-6 Å away from the center, nucleus appears to be devoid of structure. A spectrum of the other member of the pair, NGC 5930, obtained at the same resolution in wavelength, does not show components in the wings of the lines. The components we have found in the line profiles of the NGC 5929 nucleus can be interpreted as evidence for radial motion of gaseous masses at speeds of 200-300 km/sec. “Thus the NGC 5929 nucleus is evidently experiencing a mild form of activity, quite different from the activity in Seyfert nuclei”...

TABLE I. Spectrophotometric Parameters

Parameter	H ⁺		O ⁰		S ⁺		N ⁺		O ⁺⁺	
	λ4861	λ6563	λ6300	λ6363	λ6717	λ6731	λ6548	λ6584	λ4959	λ5007
W_{λ}	6.0	17	6.5	2.5	8.5	7.5	8.0	18	9.0	20
$I_{\lambda}/I_{H\beta}$	1	5.45	2.0:	0.6:	3.47	2.66	1.95	3.75	1.59	3.64
$I_{\lambda}^0/I_{H\beta}^0$	1	2.88	1.0:	0.3:	1.80	1.41	1.07	2.02	1.50	3.32
$\lg X_i/H^+ \pm 12.00$	—		7.59		7.15		7.23		8.50	

The Ly_c-radiation of ca. 1000 young hot stars O5 V class in the nucleus of the galaxy is the most probable source of gas ionization.

1982, Huchra, J. P.; Wyatt, W. F.; Davis, M.; “New bright Seyfert Galaxies”.

First time NGC 5929 classified as SyG type 2.

1984, Kennicutt, R. C., Jr.; Keel, W. C.

“Induced nuclear emission-line activity in interacting spiral galaxies”.

The authors have investigated the effect of close galaxy-galaxy interactions on the level of nuclear activity in spiral galaxies... *Galaxies with nearby companions possess significantly higher nuclear emission-line luminosities and equivalent widths, and their nuclei exhibit a significantly higher level of ionization on average. A much higher fraction of galaxies with Seyfert or Seyfert-type nuclei is found in the sample of multiple systems...* The radio and optical results make a strong case for the presence of environmentally influenced nuclear activity in a significant fraction of spiral galaxies... In any case, it is clear that *conditions in the nuclei are not isolated from the outer disks.*

1985, Keel W.C.; “Dual emission-line regions in the Seyfert galaxy NGC 5929”.

Several theoretical and empirical studies suggest that *multiple distinct emission regions exist in the nuclei of some active galaxies.* Here I show that *the type 2 Seyfert nucleus of NGC5929 contains two emission regions situated symmetrically about the centre of the galaxy...and ionization levels normally associated with Seyfert nuclei.* This system furnishes a very clear example of the presence of phenomena related to the presence of a central engine, but located at a significant distance from the ultimate source of energy. The existence of such objects suggests that the usual radiatively powered, nearly symmetric models for active nuclei may be misleading in many objects.

1986, Whittle, M.; Haniff, C. A.; Ward, M. J.; Meurs, E. J. A.; Pedlar, A.; Unger, S. W.; Axon, D. J.; Harrison, B. A.; “Extended forbidden O III emission associated with nuclear radio lobes in the Seyfert galaxy NGC 5929”.

NGC 5929 is a nearby Seyfert 2 galaxy with particularly simple double-lobed radio structure. The [OIII] emission-line distribution closely matches that of the radio emission, showing two distinct components of different velocity straddling the optical nucleus. The Narrow Line Region (NLR) of Seyfert galaxies appears to be closely related to the nuclear non-thermal radio emission. ... The observations we have presented clearly demonstrate *a close association between the radio-emitting region and the [O III]-emitting region (NLR).* ... *The absence of a young stellar population is evident from the 5150 Å continuum image,* which shows no enhancement in the vicinity of the radio lobes. Similarly a low-dispersion spectrum taken through a 4.7-arcsec circular aperture by Kennicutt & Keel (1984) shows *a red continuum with absorption lines characteristic of an old population.*

1988, Ken-Ichi Wakamatsu & Mitsugu T. Nishida

"Dual Emission-Line Clouds In The Nuclei Of The Interacting Pair Arp 90" + Addendum.

On optical spectra, dual-peak emission-line clouds have been discovered in both nuclei of an interacting pair Arp 90 (NGC 5929 + NGC 5930). The clouds in each galaxy are quite similar in their spatial, kinematical, and radio properties, but quite different in the excitation levels of the ionized gas, i.e., classified as H II region type for NGC 5930 or Seyfert 2 type for NGC 5929. NGC 5930 was detected as an IRAS source with the luminosity $L_{IR} = 2.0 \times 10^{10} L_{sun}$, while NGC 5929 was not. The authors have detected 2.6 mm CO (J = 1-0) line emission from the nuclear region of NGC 5930 but not from NGC 5929.

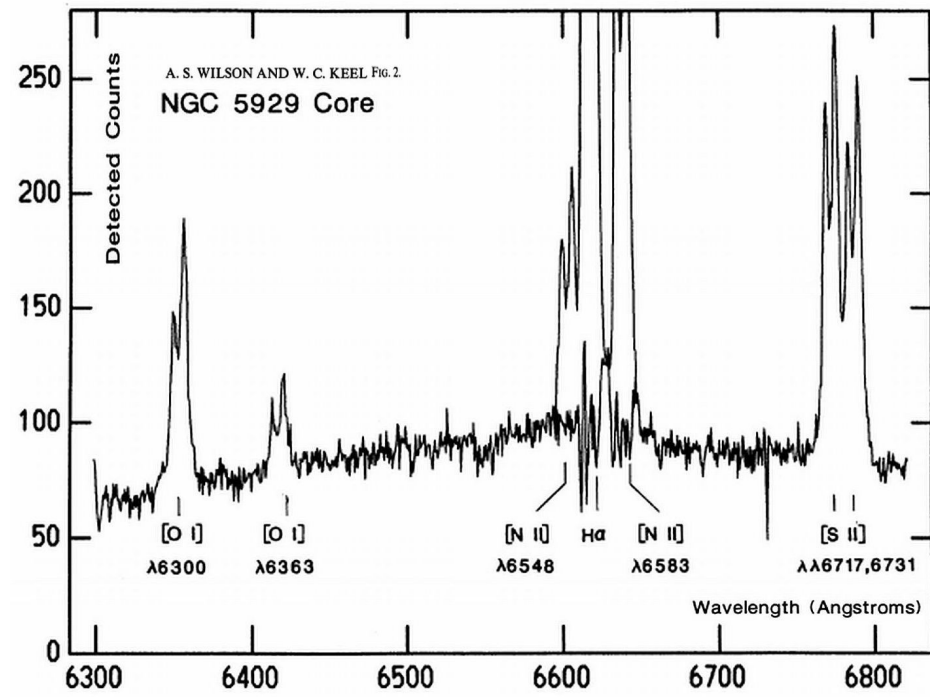
1989, D. Taylor, J. E. Dyson, D. J. Axon and A. Pedlar

“A plasmon driven bowshock model for the narrow line region of NGC 5929”.

We describe *a model for the narrow line region (NLR) of Seyfert nuclei, in which the linear motion of radio-emitting bubbles of plasma ejected from the nucleus drives bowshocks into the ambient nuclear medium.* The cooled shocked gas, photo-ionized by the UV nuclear continuum, produces the optical NLR emission. ***The NGC 5929 galaxy has two nuclear components at both radio and optical wavelengths, which we model as two plasmon driven bowshocks on either side of the nucleus.***

1989, Andrew S. Wilson & William C. Keel; “High-Resolution Observations Of The Multicomponent Nucleus of NGC 5929”.

The central region of the Type 2 Seyfert galaxy NGC 5929 is known to contain double radio-continuum and optical emission-line clouds separated by ~1". When the radio continuum and [O III] 5007 image of Whittle et al. are compared at the same spatial resolution, there is no evidence that the separations or position angles of the radio and emission-line clouds differ. The double H_α clouds appear to differ in position angle by ~20deg from the radio lobes.



1991, Afanas'ev, V. L.; Sil'chenko, O. K.;

“Gas kinematics in the central regions of Seyfert galaxies. IV. NGC 5929”.

Two gas clouds being the main forbidden line emitters in the center of NGC 5929 are found to possess the relative line-of-sight velocities -50 km/s (the eastern cloud) and +270 km/s (the western cloud). The emission brightness centers which coincide with the radio lobes are probably the shock wave regions forming on the border between the clouds and the galactic disk.

1993, Bower, G. A.; Wilson, A. S.; Mulchaey, J. S.; Miley, G. K.; Heckman, T. M.; Krolik, J. H.

“HST Images of the Seyfert Galaxy NGC 5929 and Its Companion NGC 5930”.

The nuclei of both galaxies contain emission line gas. Previous *ground-based observations of the Seyfert galaxy NGC 5929 include [O III] and H α + [N II] images, showing that its nucleus contains an elongated region of high-excitation emission line gas. In these HST images, this gas is clearly separated into two distinct regions separated by about 1" . These observations of Arp 90 present an opportunity to examine the details of the possible role of galaxy interactions in the triggering of an AGN.*

1994, Gary A. Bower, Andrew S. Wilson, John S. Mulchaey, George K. Miley, Timothy M. Heckman and Julian H. Krolik

“Hubble Space Telescope Images Of The Seyfert Galaxies Ngc 5929 And MCG 8-11-11”.

The high-excitation gas in the narrow line region (NLR) of NGC 5929 is resolved into individual clouds in the central 1.5". Although the [O III] emission is clearly not spherically symmetric with respect to the nucleus, it does not define a distinct "bicone" morphology, as observed by the HST in a few other Seyfert galaxies.

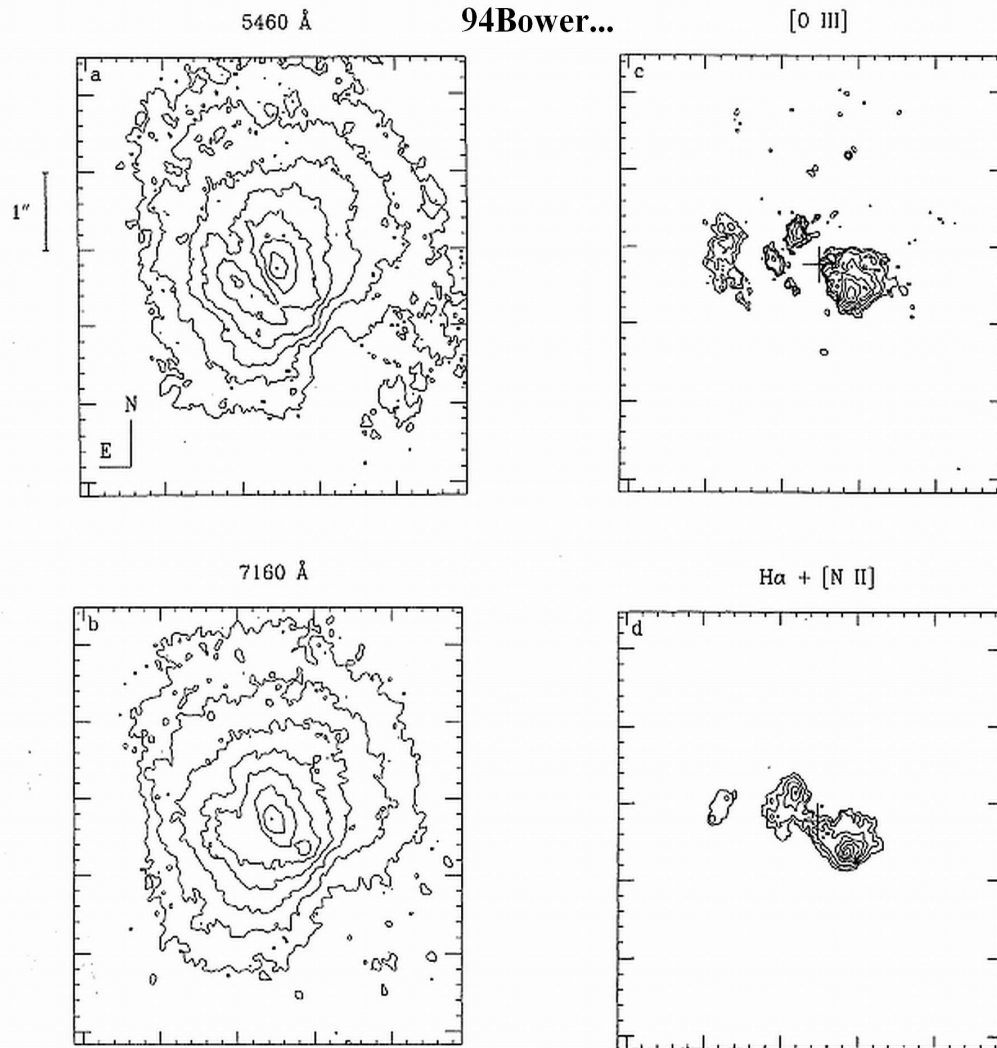


FIG. 1. Contour plots of the deconvolved *HST* Planetary Camera images of the nuclear region of the type 2 Seyfert galaxy NGC 5929. The plots have a resolution of $0''.1$, and the contour interval is 0.5 mag. The nucleus is taken as the position of the continuum peak. The location of the nucleus in each emission line image is marked by a cross in both Figs. 1 and 2. (a) The green continuum image; contours range from 6.5×10^{-17} to 1.5×10^{-15} $\text{erg cm}^{-2} \text{s}^{-1} \text{\AA}^{-1} \text{arcsec}^{-2}$. (b) The red continuum image; contours range from 8.1×10^{-17} to 2.1×10^{-15} $\text{erg cm}^{-2} \text{s}^{-1} \text{\AA}^{-1} \text{arcsec}^{-2}$. (c) The [O III] image; contours range from 1.8×10^{-14} to 4.7×10^{-13} $\text{erg cm}^{-2} \text{s}^{-1} \text{arcsec}^{-2}$. (d) The $\text{H}\alpha + [\text{N II}]$ image; contours range from 1.0×10^{-14} to 1.0×10^{-12} $\text{erg cm}^{-2} \text{s}^{-1} \text{arcsec}^{-2}$.

We find no direct evidence for the reddening and/or obscuration effects characteristic of a dusty torus, which, in the context of "unified models", is expected to obscure the active galactic nucleus (AGN) in type 2 Seyfert galaxies. The correspondence between the emission line gas and the radio morphology suggests that the structure of the NLR in NGC 5929 is governed by matter ejected from the AGN. A comparison of the recombination rate of hydrogen in the brightest emission line cloud with an upper limit on the ionizing luminosity emitted toward Earth provides no evidence that the central ionizing source radiates anisotropically.

1996, B. M. Su, T. W. B. Muxlow, A. Pedlar, A. J. Holloway, W. Steffen, M. J. Kukula and R. L. Mutel; “Compact radio structure in the Seyfert nucleus of NGC 5929”.

We confirm the triple structure reported in earlier studies. The weak central source of the triplet is almost certainly associated with the active nucleus... *We compare the radio structure of NGC 5929 to recent HST images and discuss the possible models to relate the radio and optical structures (bowshock model (Taylor et al. 1989), plasmon model (Pedlar et al. 1985)).*

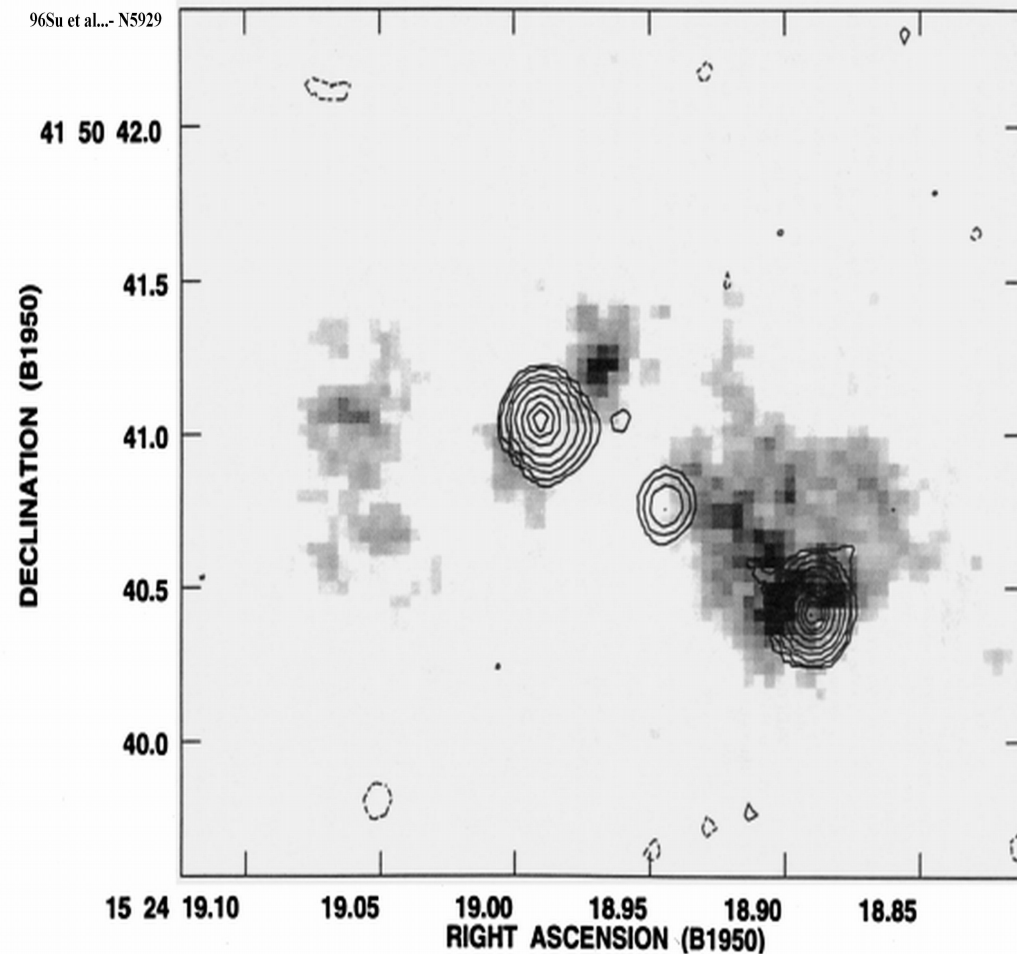


Figure 7. A contour map at 1.6-GHz superimposed on the [O III] image from the *HST*. The radio map has been restored with a 0.125×0.122 arcsec² beam (PA = $-15^\circ 46'$). The contours are -2, -1, 1, 2, 4, 8, 16, 32, 50, 64, 80 and 99 per cent of the peak brightness, which is $21.8 \text{ mJy beam}^{-1}$. The images have been registered by aligning the peak of the optical continuum with the central radio component.

1997, Ferruit, P.; Wilson, A. S.; Mulchaey, J.; Ferland, G.; Whittle, M.; Simpson, C.

“Off-nucleus HST/FOS spectra of the two Seyfert galaxies NGC 5929 and NGC 2110”.

As many others, the two Seyfert 2 galaxies NGC 5929 and NGC 2110 display bright extranuclear regions of line emission which are spatially associated with radio jets or lobes. The nature of the excitation and ionization mechanisms of this line emitting gas (shocks induced by the propagation of the radio ejecta, photoionization by the nuclear radiation...) remain very uncertain. **Recent modelings either of shock excitation (e.g. Dopita & Sutherland, 1995) or nuclear photoionization (e.g. Binette, Wilson & Storchi-Bergmann, 1996) have stressed the importance of using UV lines diagnostic in addition to the classical optical ones to distinguish between these two families of mechanisms.**

1997, Ferruit, P.; Pecontal, E.; Wilson, A. S.; Binette, L.

“Sub-arcsecond resolution 2D (x,y,lambda) spectrography of the emission line region of NGC 5929 with TIGER”

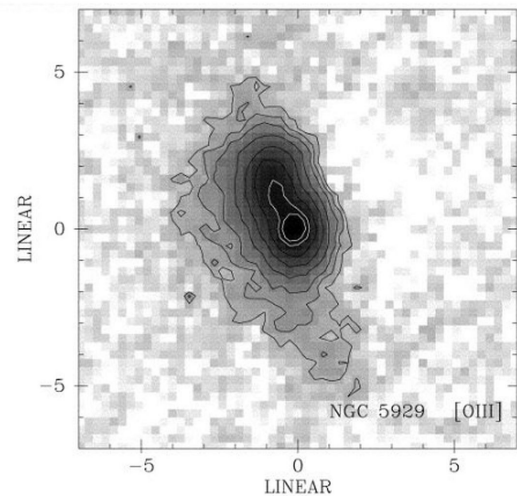
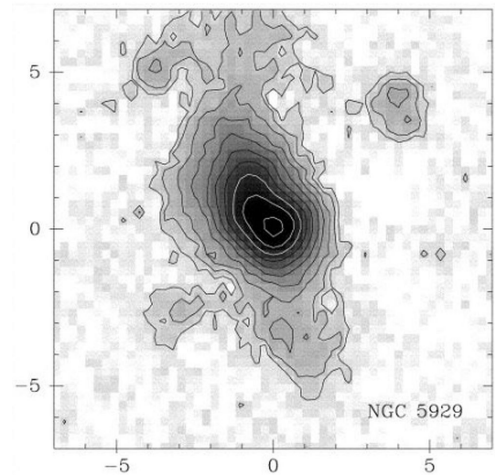
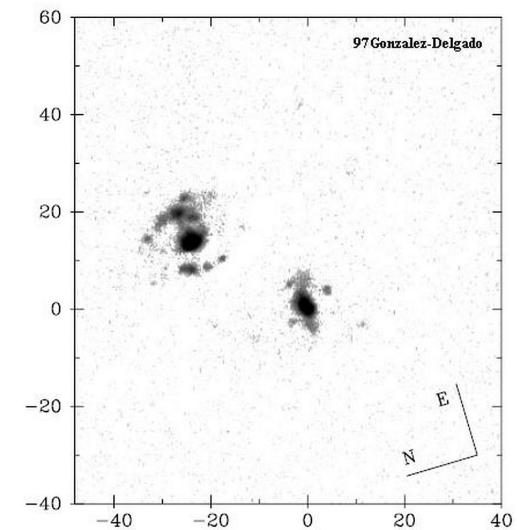
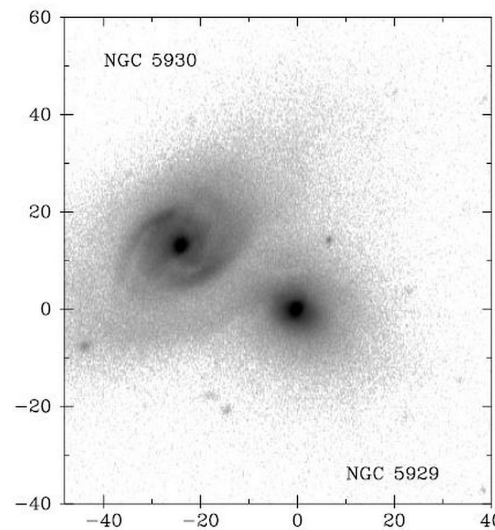
...We report observations of the *Seyfert 2 galaxy NGC 5929* with the integral field spectrograph Tiger. These 2D spectrographic data, with sub-arcsecond spatial resolution, consist of **394 flux-calibrated spectra, covering the [NII] , Halpha and [SII] emission associated with the two radio-lobes. The two optical line emission components have been kinematically separated using Gaussian fitting of the spectra. ... All models predict edge-brightened bow shock or cylindrical shell structures for the ionized gas, which seems to conflict with the HST imaging.**

High spatial resolution spectrography (e.g. with STIS) of NGC 5929 is needed to obtain the velocity structure of both the NE and SW components and to understand the relationship between the relativistic and thermal gases. Models of jet-ambient medium interactions with more extensive coverage of parameter space are also desirable.

1997, Rosa M. Gonzalez Delgado, Enrique Perez, Clive Tadhunter, Jose M. Vilchez, and Jose Miguel Rodriguez-Espinosa; “H II Region Population In A Sample Of Nearby Galaxies With Nuclear Activity. I. Data And General Results”.

NGC 5929/C 5930: This interacting pair is formed by an S2 nucleus, NGC 5929, in an Sab galaxy and a starburst nucleus in an Sb galaxy, NGC 5930.

The emission-line morphology in the two disks are very different. NGC 5929 only shows some weak H II regions ; however, the disk of NGC 5930 shows bright H II regions, mainly along the spiral arms.



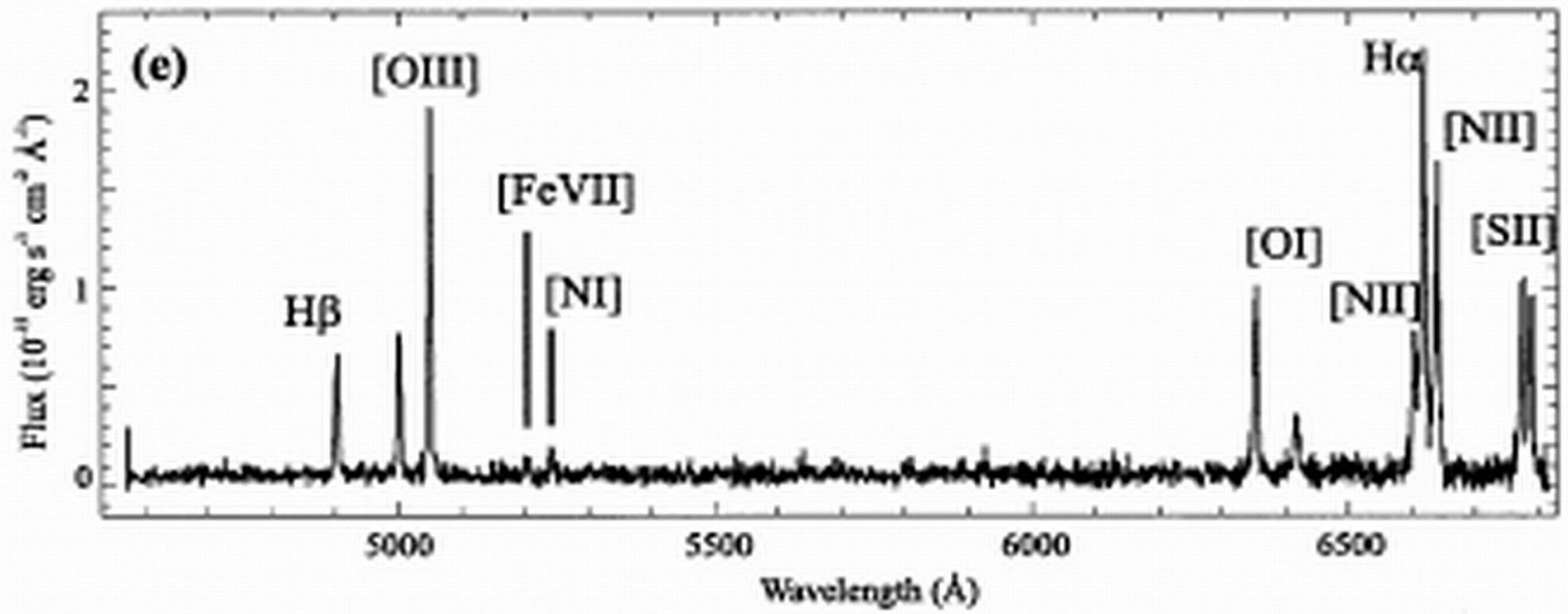
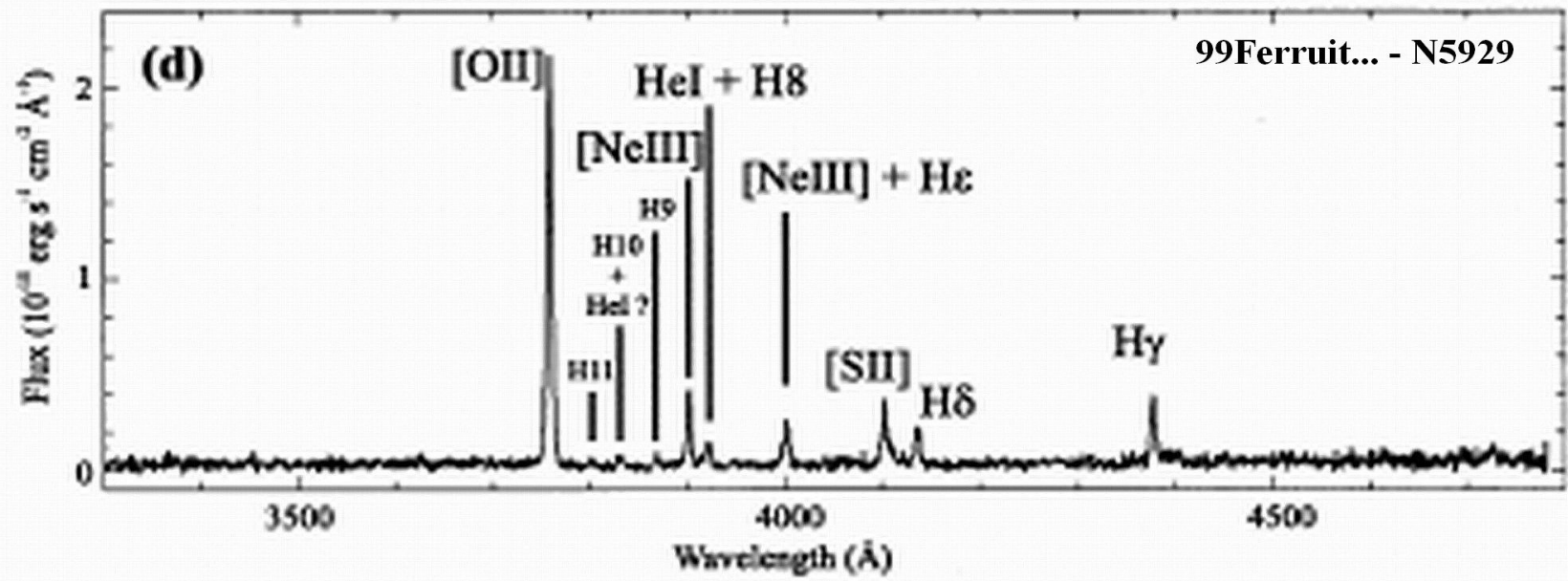
1998, Kotilainen J.K.; “Optical colour maps of Seyfert galaxies. II. More Seyfert 2s”.

... we detect **extended blue continuum components in the circumnuclear region** of several galaxies. **These components** are either elongated (in Mkn 533, Mkn 607, Mkn 1066, NGC 5347, NGC 5953 and NGC 7319) or **form a double structure across the nucleus (in NGC 5929)**. **NGC 5929** is an Sab pec galaxy interacting with the starburst galaxy NGC 5930, together forming the galaxy pair Arp 90. **NGC 5929** has a **faint hard X-ray spectrum**, implying heavy absorption. It has **triple radio structure**. **The [OIII] emission resembles closely the radio morphology**. ...The nucleus of NGC 5929 is situated between two blue maxima at opposite sides of the nucleus... they possibly represent extranuclear scattering mirrors of anisotropically escaping nuclear light.

1999, Pierre Ferruit, Andrew S. Wilson, Mark Whittle, Chris Simpson, John S. Mulchaey and Gary J. Ferland; “Hubble Space Telescope/Faint Object Spectrograph Spectroscopy Of Spatially Resolved Narrow-Line Regions In The Seyfert 2 Galaxies NGC 2110 and NGC 5929”.

NGC 5929 is a member of an interacting pair with NGC 5930 (Arp 90) and hosts a Seyfert 2 nucleus. It displays an **extended emission-line region with two main components**, one blueshifted and one redshifted, located northeast and southwest of the nucleus, respectively. Radio observations show **a triple radio source with two lobes** straddling an unresolved nuclear component. Comparison between the radio maps and the emission-line observations reveals **a close morphological and kinematical association between the ionized gas and the radio-emitting material**.

We have obtained **spectra of the brightest region of the southwest emission-line cloud of NGC 5929**. **The observed line ratios are compared with the predictions of the two component (matter- and ionization-bounded, MB-IB), central source photoionization models of Binette, Wilson, & Storchi-Bergmann and of the fast, photoionizing (“autoionizing”) shock models of Dopita & Sutherland**. **In NGC 5929, the MB-IB models have problems reproducing the strengths of the neon lines, while shock/precursor models with a velocity $\sim 300 \text{ km s}^{-1}$ provide a good match to the data**.



1999, Paul Martini And Richard W. Pogge; “Hubble Space Telescope Observations Of The Cfa Seyfert 2 Galaxies: The Fueling Of Active Galactic Nuclei”.

An estimate of the gas density in the nuclear spirals, based on extinction measurements, suggests that *the nuclear spiral dust lanes are probably shocks in nuclear gas disks that are not strongly self-gravitating. Since shocks can dissipate energy and angular momentum, these spiral dust lanes may be the channels by which gas from the host galaxy disks is being fed into the central engines.* **NGC 5929 has a distinct nuclear bar in the near-infrared images, but it is hidden by dust in the visible-light images.** The V-H color map of this galaxy shows the nuclear region is very dusty, with an irregular dust morphology.

2000, Rhee, Joseph H.; Larkin, James E.

“Probing the Dust Obscuration in Seyfert Galaxies Using Infrared Spectroscopy”.

The Seyfert 2 galaxy, NGC 5929, consistent with dust being present on larger scales, shows significant obscuration to the narrow-line region.

2001, Rosa M. Gonzalez Delgado, Timothy Heckman and Claus Leitherer

“The Nuclear and Circumnuclear Stellar Population in Seyfert 2 Galaxies: Implications for the Starburst-Active Galactic Nucleus Connection”.

...Our goal is to **search for the direct spectroscopic signature of massive stars and thereby probe the role of circumnuclear starbursts in the Seyfert phenomenon.** The method used is based on the detection of the **higher order Balmer lines and He I lines in absorption** and the **Wolf-Rayet feature at ~4680 Å in emission.** *These lines are strong indicators of the presence of young (a few Myr) and intermediate-age (a few 100 Myr) stellar populations...* We consider the possibility that **there may be two distinct subclasses of Seyfert 2 nuclei ("starbursts" and "hidden broadline regions" [BLRs]).** **Cont...**

... *Most of the nuclei of our sample can be grouped in two classes, those with young and intermediate age stars and those with an optical continuum dominated by old stars.* This segregation in two groups poses an important question: *are there two different classes of S2 nuclei?*

Objects with a continuum dominated by an old stellar population (Mrk 3, Mrk 34, Mrk 348, Mrk 573, NGC 1386, NGC 2110, **NGC 5929**, and NGC 7212 - *the stellar lines are similar to those of an old population.*

2001, R. Cid Fernandes, T. Heckman, H. Schmitt, R. M. Gonzalez Delgado and T. Storchi-Bergmann; “Empirical Diagnostics of the Starburst-AGN Connection”.

Rem.: Here “composite” and “pure” are “types” of nature of the galaxies...!!!

...we examine a variety of *more easily measured quantities* for this sample, such as *the equivalent widths of strong absorption features, continuum colors, emission line equivalent widths, emission line ratios and profiles, far-IR luminosities, and near-UV surface brightness.* We compare *the composite starburst + Seyfert 2 nuclei* to *“pure” Seyfert 2 nuclei, Starburst galaxies, and normal galactic nuclei.* We show that *starbursts do indeed leave clear and easily quantifiable imprints on the near-UV to optical continuum and emission line properties of Seyfert 2's.* **Composite starburst + Seyfert 2 systems can be recognized by:**

- (1) *a strong “featureless continuum”* (FC), which dilutes the Ca II K line from old stars in the host's bulge to an equivalent width $W_{K} < 10 \text{ \AA}$;
- (2) *emission lines* whose equivalent widths are intermediate between starburst galaxies and “pure” Seyfert 2's;
- (3) *relatively low excitation line ratios*, which indicate that part of the gas ionization in these Seyfert 2's (typically ~50% of H β) is due to photoionization by OB stars;
- (4) *large far-IR luminosities* ($> \sim 10^{10} L_{\text{sun}}$);

(cont. on next page...)

(5) *high near-UV surface brightness* ($\sim 10^3 \text{ L}_{\text{sun}} \text{ pc}^{-2}$).

...**"pure" Seyfert 2's**. This denomination is used simply to indicate that no clear signs of starburst activity have been detected in our previous studies (e.g., NGC 1358 and **NGC 5929**).

...a substantial fraction of our *composites* (9 of 15) are associated with interacting systems or groups. The analogous fraction for the *"pure"* Seyfert 2's is only 4 out of 20 (Mrk 348, Mrk 607, **NGC 5929**, and NGC 7212).

We find stellar nuclear bar candidates for nearly 20% of the total sample and **the dust lanes in Mrk 471 and NGC 5929 exhibit a more complex morphology (NGC 5929 do not have known largescale bar)**. *The fact that most of these AGNs do not appear to contain stellar nuclear bars suggests that they are not the fueling mechanism for most low-luminosity AGNs.*

...**The circumnuclear region of NGC 5929 is quite irregular.**

2003, D. Raimann, T. Storchi-Bergmann, R. M. Gonzalez Delgado, R. Cid Fernandes, T. Heckman, C. Leitherer and H. Schmitt

Stellar population gradients in Seyfert 2 galaxies: northern sample

...In order to characterize the stellar population and other continuum sources (e.g. featureless continuum, FC) we have measured the equivalent width, W , of six absorption features, four continuum colours and their radial variations, and performed spectral population synthesis as a function of distance from the nucleus. About half of the sample has Ca II K and G band W values smaller at the nucleus than at 1 kpc from it, owing to a younger population and/or FC.

NGC 5929 is in a group dominated by 10-Gyr metal-rich stellar population (with solar or above metallicity).

2007, N. Jackson and R. J. Beswick

“Near-infrared spectra of Seyfert galaxies and line production mechanisms”.

New observations are reported of J-band spectra (1.04 μm – 1.4 μm) of three Seyfert 2 galaxies, Mkn 34, Mkn 78 and *NGC 5929*. ***A possible detection of extranuclear [PII] emission suggests, if real, that photoionization by the active nucleus is the dominant line excitation mechanism over the whole source, including the regions coincident with the radio jet.***

2009, Wang, Jian-Min; Chen, Yan-Mei; Hu, Chen; Mao, Wei-Ming; Zhang, Shu; Bian, Wei-Hao

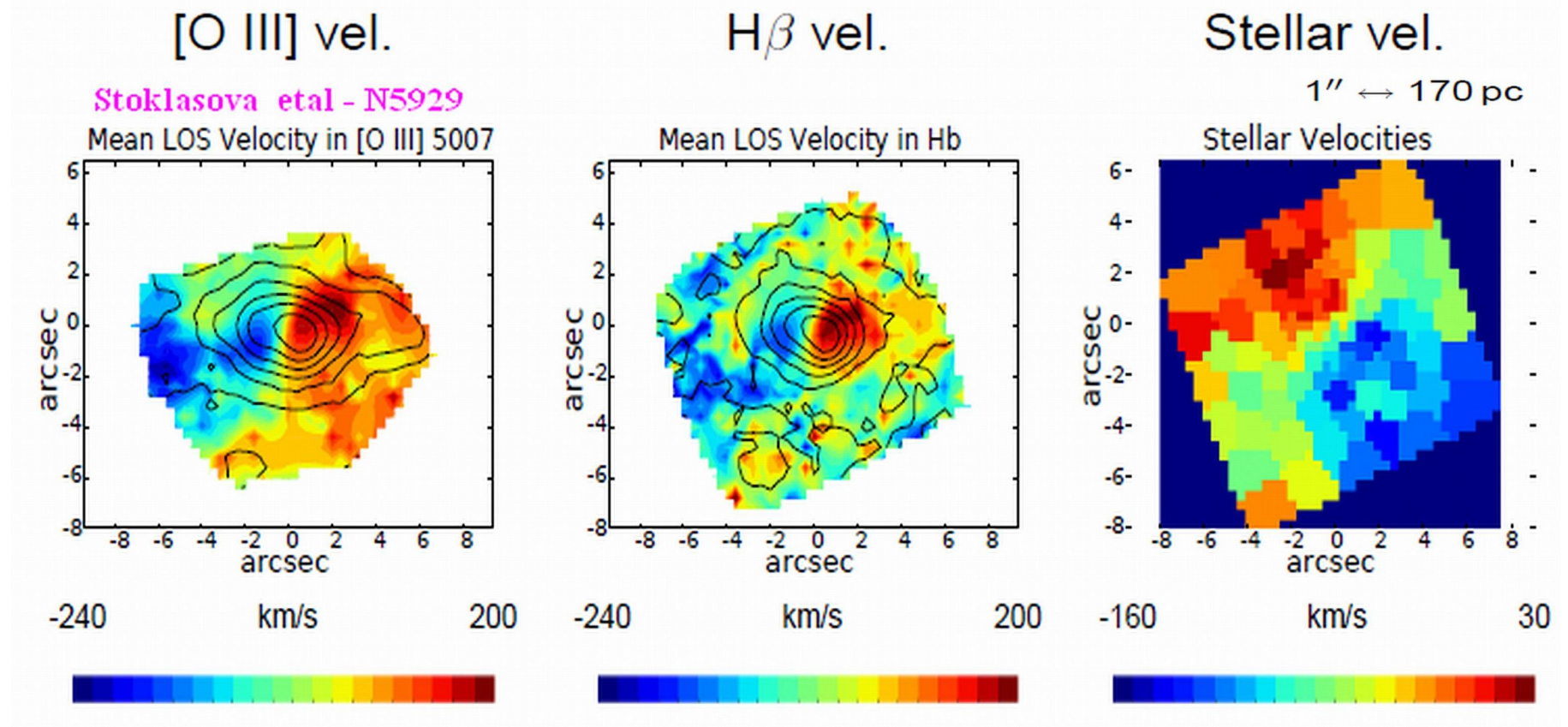
“Active Galactic Nuclei with Double-Peaked Narrow Lines: Are they Dual Active Galactic Nuclei?”

Double-peaked [O III] profiles in active galactic nuclei (AGNs) may provide evidence for the existence of dual AGNs, but a good diagnostic for selecting them is currently lacking. Starting from ~7000 active galaxies in Sloan Digital Sky Survey DR7, we assemble **a sample of 87 type 2 AGNs with double-peaked [O III] profiles.** The nuclear obscuration in the type 2 AGNs allows us to determine redshifts of host galaxies through stellar absorption lines. ***We typically find that one peak is redshifted and another is blueshifted relative to the host galaxy. We find a strong correlation between the ratios of the shifts and the double peak fluxes.*** The correlation can be naturally explained by the Keplerian relation predicted by models of co-rotating dual AGNs. ***The current sample statistically favors that most of the [O III] double-peaked sources are dual AGNs and disfavors other explanations, such as rotating disk and outflows.***

2010, D.J. Rosario, M. Whittle, C.H. Nelson, A.S. Wilson

‘The Radio Jet Interaction In Ngc 5929: Direct Detection Of Shocked Gas’.

We report the discovery of *kinematic shock signatures associated with a localized radio jet interaction in the merging Seyfert galaxy NGC 5929*. We explore the velocity-dependent ionization structure of the gas and find that *low ionization gas at the interaction site is significantly more disturbed than high ionization gas, which we attribute to a local enhancement of shock ionization due to the influence of the jet*. The characteristic width of the broad low-ionization emission is consistent with shock velocities predicted from the ionization conditions of the gas.



On the next few slides some results from the previous investigations of NGC 5929 are presented:

- **1995, Nelson... redshift measurements from stars, HI, [OIII] and [SIII] lines**
- **1996, Schmidt... some basic parameters – distance, line fluxes, luminosities, morphology etc.**
- **2001, Gonzalez-Delgado... equivalent width of H_β and some stellar absorption lines**
- **1986, Whittle... fluxes and separation of the components, radial velocities etc.**
- **1992, Kennicutt... equivalent width and fluxes of some emission lines**
- **1993, Osterbrock... measured and corrected emission-line ratios**
- **1997, Alonso-Herrero... [OIII] and near-IR fluxes and luminosities, visual extinction etc.**
- **1997, Ferruit... integrated properties of NE and SW components**
- **1988, Wakamatsu... equivalent widths for red and blue components of NGC 5929/NGC 5930**
- **1999, Ferruit... emission line fluxes and some models**

95Nelson - Tabl.4

REDSHIFTS: [O III], [S III], STARS, AND H I

Name (1)	[OIII]		[SIII]	Stars			Pub. (8)	Ref. (9)	HI		
	Med. (2)	C80 (3)	C80 (4)	Ca T (5)	Mg b (6)	Combined (7)			α (10)	Profile (11)	Ref. (12)
37 NGC 5929	2550 \pm 3	2593 \pm 15	...	2511 \pm 22	2490 \pm 8	2492 \pm 8	2581 \pm 15	2PS	14

96Schmidt - Tabl.2

SAMPLE PROPERTIES

Object ^a	Morphological Type ^b	Distance ^c	Scale ^d	$\log(F_{[OIII]})^e$	$\log(L_{[OIII]})^f$	PA ^g	i^h	$\log[F(Lim)]^i$	$\log[L(Lim)]^j$
NGC 5929.....	Sub:pcc	35.8	173.6	-13.03	40.16	\approx fo	26	1.677	37.41

EQUIVALENT WIDTHS (IN Å UNITS) OF THE H β EMISSION-LINE AND THE STELLAR ABSORPTION LINES Ca II K λ 3918, G-BAND AND THE CALCIUM TRIPLET AT λ 8498, 8542, AND 8662

01Gonzalez-Delgado

Name	H β Emission	Ca II K	G Band	Ca II λ 8498	Ca II λ 8542	Ca II λ 8662
NGC 5929	14.0 \pm 0.7	11 \pm 1.0	7.1 \pm 0.7	1.3 \pm 0.2	3.0 \pm 0.2	2.2 \pm 0.2

Table 2. [OIII] component properties. 86Whitle

	NE	(both)	SW	
1 Separation (PA 60; Long-Slit)		0.95 \pm 0.11 arcsec ; 242 \pm 28 pc		1
2 Separation (Image)		0.76 \pm 0.14 arcsec ; 193 \pm 36 pc		2
3 Nuclear Distance (PA 60)	0.38 \pm 0.11 arcsec ; 97 \pm 28 pc		0.57 \pm 0.07 arcsec ; 145 \pm 18 pc	3
4 Component PA (Image)		63 \pm 2 deg		4
5 Diffuse Emission PA (Image)		80 \pm 5 deg		5
6 Heliocentric Velocity (km s ⁻¹)	2310 \pm 10		2625 \pm 15	6
7 Velocity Difference (km s ⁻¹)		315 \pm 18		7
8 FWHM (km s ⁻¹)	80 \pm 10		185 \pm 20	8
9 Log F ₅₀₀₇ (erg s ⁻¹ cm ⁻²)	-13.41		-13.06	9
10 Log L ₅₀₀₇ (erg s ⁻¹)	40.15		40.48	10
11 F ₅₀₀₇ /F _{HB}	3.1 \pm 0.2		4.5 \pm 0.2	11

92Kennikut - tabl.2

LOW-RESOLUTION DATA

NAME (1)	TYPE (2)	APERTURE (3)	41-50 (4)	EQUIVALENT WIDTH (Å)					FLUX (H α + [N II] = 1)					NOTES (15)
				[O II] (5)	H β (6)	[O III] (7)	H α + [N II] (8)	[S II] (9)	[O II] (10)	H β (11)	[O III] (12)	[S II] (13)	[N II]/H α (14)	
NGC 5929	Sbcp	45	0.78	40	0	12	29	12	0.25	...	0.34	0.45	0.55	1,6

93Osterbrock

TABLE 6

LOGARITHMS OF MEASURED AND CORRECTED EMISSION-LINE RATIOS:^a LOW DISPERSION DATA

Object	H β (n)	[O III] λ 5007	[O I] λ 6300	[N II] λ 6548	H α n	[N II] λ 6583	[S II] λ 6724	r c
NGC 5929	-0.17	0.43	-0.06	-0.13	0.55	0.34	0.40	...
	-0.15	0.42	-0.24	-0.34	0.34	0.12	0.18	0.68

^a Normalized with respect to [O III] λ 4959.

93Osterbrock - Tabl.7

LOW-DISPERSION DATA

Object	He II λ 4686	[N I] λ 5199	[Fe VII] λ 6087	Blend λ 6364	[O I] λ 6364	[Fe X] λ 6375
NGC 5929	-0.42	-0.54	-1.05
	-0.61	-0.73	-1.24

^a Normalized with respect to [O III] λ 4959.

Table 1. Near-IR photometry and [O III] λ 5007 fluxes and luminosities for the Seyfert 2 sample.

97Alonso-Herrero

Galaxy (1)	v_{hel} (km s $^{-1}$) (2)	$\log f_{\text{O III}}$ (3)	$\log f_K$ (4)	$K/\text{O III}$ (5)	$\log f_L$ (6)	$L/\text{O III}$ (7)	$\log l_{\text{O III}}$ (8)	$\log l_L$ (9)	O III ref (10)	K, L ref (11)
NGC 5929	2561	-13.03	-11.09	87.1	-11.21	66.1	40.47	42.29	1	4, 3"

Table 10. Visual extinctions for the Seyfert 2s.

Galaxy	$A_V(\text{[O III]})$	$A_V(\text{HX})$	$A_V(N_H)$
NGC 5929	>37	no	no

Table 1. Integrated properties of the NE and SW components. The FWHMs have been corrected for the 3.9 Å instrumental broadening. The densities have been derived from the [S II] λ 6716/[S II] λ 6731 line ratio, assuming $T = 10^4$ K.

	$v - 2492$ km s $^{-1}$	FWHM km s $^{-1}$	H α erg s $^{-1}$	[N II] λ 6583 erg s $^{-1}$	[S II] λ 6716 erg s $^{-1}$	[S II] λ 6731 erg s $^{-1}$	n cm $^{-3}$	[N II]/H α ¹	[S II]/H α ²
NE	-145	180	$1.95 \cdot 10^{39}$	$1.14 \cdot 10^{39}$	$0.74 \cdot 10^{39}$	$0.57 \cdot 10^{39}$	130	0.6	0.7
SW	+115	220	$2.48 \cdot 10^{39}$	$1.75 \cdot 10^{39}$	$1.00 \cdot 10^{39}$	$0.94 \cdot 10^{39}$	450	0.7	0.8

¹ [N II] λ 6583 / H α ² ([S II] λ 6716 + [S II] λ 6731) / H α

97Ferruit...

Table 2. Spectral characteristics of the B+C, D and E components of the NE lobe. Velocities are given in km s $^{-1}$. [N II]₂ corresponds to [N II] λ 6583, [S II]₁ to [S II] λ 6716 and [S II]₂ to [S II] λ 6731.

ID	$v - 2492$	[N II] ₂ /H α	[S II] ₁₊₂ /H α	[S II] ₁ /[S II] ₂
B+C	-175	0.47 ± 0.02	0.48 ± 0.06	1.16 ± 0.13
D	-175	0.84 ± 0.06	0.9 ± 0.2	1.03 ± 0.15
E	-140	0.7 ± 0.1	0.9 ± 0.3	1.2 ± 0.3

EQUIVALENT WIDTHS OF EMISSION LINES OF BLUE AND RED
COMPONENTS^a

LINE	NGC 5930		NGC 5929	
	Blue	Red	Blue	Red
H β λ 4861		7.2 ^b	4.0	4.4
[O III] λ 4959	4.1	5.1
[O III] λ 5007		3.0 ^b	17	23
[N I] λ 5199	Trace	
[O I] λ 6300	3.0	7.0
[O I] λ 6363	Trace	
[N II] λ 6548	8.0	8.0	4.5	4.5
H α λ 6563	41	41	24	30
[N II] λ 6583	24	24	12	21
[S II] λ 6717	6.0	6.0	8.0	12
[S II] λ 6731	4.5	4.5	6.0	9.0

^a Averaged over the region 3".6 along the slit and given in angstrom units. Errors are ~20% or 40% for lines larger or smaller than 10 Å, respectively.

99Ferruit - Tabl.5

LINE FLUXES FOR NGC 5929 (see § 3.4)

Line(s)	Flux ^a	$F/F_{H\beta}$ ^b ($A_V = 0$ mag)	$F/F_{H\beta}$ ^c ($A_V = 0.6$ mag)	$F/F_{H\beta}$ ^c ($A_V = 0.9$ mag)	$F/F_{H\beta}$ ^c ($A_V = 1.2$ mag)
[O II] $\lambda\lambda 3726, 3729$	14.8 ± 0.3	340 ± 50	410 ± 60	460 ± 70	510 ± 80
[Ne III] $\lambda 3869$	2.21 ± 0.26	50 ± 13	61 ± 15	67 ± 17	73 ± 19
He I $\lambda 3889 + H8$	0.81 ± 0.20	18 ± 7	22 ± 8	24 ± 9	27 ± 10
[Ca II] $\lambda 3934$	< 0.2	< 5	< 6	< 7	< 8
[Ne III] $\lambda 3969 + He$	1.6 ± 0.3	36 ± 12	43 ± 14	47 ± 15	51 ± 17
[S II] $\lambda\lambda 4069, 4077$	2.0 ± 0.4	45 ± 15	53 ± 18	57 ± 19	62 ± 21
H δ	1.09 ± 0.22	25 ± 8	29 ± 10	31 ± 10	33 ± 11
H γ	1.73 ± 0.27	39 ± 11	43 ± 13	46 ± 13	48 ± 14
[O III] $\lambda 4363$	< 0.4	< 10	< 12	< 12	< 13
He II $\lambda 4686$	< 0.5	< 13	< 14	< 14	< 4
H β	4.4 ± 0.6	100	100	100	100
[O III] $\lambda 5007$	12.7 ± 0.9	290 ± 60	280 ± 60	280 ± 60	270 ± 60
[Fe VII] $\lambda 5158 + [Fe II]?$	0.5 ± 0.5
[N I] $\lambda\lambda 5198, 5200$	1.2 ± 0.5	27 ± 15	26 ± 14	25 ± 14	25 ± 14
[Fe VII] $\lambda 5276$	< 0.5	< 13	< 12	< 11	< 0
[N II] $\lambda 5755$	< 0.7	< 18	< 16	< 15	< 15
He I $\lambda 5876$	< 1	< 26	< 23	< 22	< 20
[Fe VII] $\lambda 5721$	< 1	< 26	< 23	< 21	< 20
[O I] $\lambda 6300$	8.2 ± 1.0	190 ± 50	160 ± 40	140 ± 40	130 ± 30
[S III] $\lambda 6310$	< 0.3	< 8	< 7	< 6	< 6
[Fe X] $\lambda 6374$	< 0.3	< 8	< 7	< 6	< 6
H α	20.6 ± 2.5	470 ± 120	390 ± 100	350 ± 90	320 ± 80
[N II] $\lambda 6583$	12.1 ± 1.6	270 ± 90	230 ± 70	210 ± 60	190 ± 60
[S II] $\lambda 6717$	7.6 ± 0.7	170 ± 40	140 ± 30	130 ± 30	115 ± 26
[S II] $\lambda 6731$	6.7 ± 0.6	150 ± 30	120 ± 30	112 ± 25	101 ± 23

NOTE.—The error bars correspond to a 90% confidence level.

^a Observed line flux in 10^{-15} ergs s^{-1} cm^{-2} .

^b Observed line flux relative to H β with $F_{H\beta} = 100$.

^c Reddening-corrected line flux relative to H β with $F_{H\beta} = 100$.

99Ferruit - Tabl.10

LINE RATIOS IN NGC 5929

Line Ratio	Observed	$V_s = 200 \text{ km s}^{-1}$	$V_s = 300 \text{ km s}^{-1}$	$V_s = 400 \text{ km s}^{-1}$	$V_s = 500 \text{ km s}^{-1}$
[O III] $\lambda 5007/\text{H}\beta$	2.1–3.5	1.52–1.58	5.9–6.5	8.0–9.1	12.5–13.8
[O II] $\lambda 3727/\text{H}\beta$	3.4–5.1	2.3–3.6	1.7–5.2	1.7–7.0	1.7–7.2
[O I] $\lambda 6300/\text{H}\alpha$	0.30–0.52	0.07–0.13	0.32–0.47	0.57–0.81	0.81–0.95
[O II] $\lambda 3727/[\text{O III}]\lambda 5007$	1–2	1.5–2.3	0.3–0.8	0.2–0.8	0.1–0.5
[O I] $\lambda 6300/[\text{O III}]\lambda 5007$	0.39–0.77	0.14–0.26	0.15–0.23	0.18–0.30	0.17–0.21
[O III] $\lambda 5007/[\text{O III}]\lambda 4363$	> 23	~28	103–108	107–109	79–82
[N II] $\lambda 6583/\text{H}\alpha$	0.42–0.75	0.19–0.41	0.23–0.65	0.34–0.86	0.39–0.85
[S II] $\lambda \lambda 6717, 6731/\text{H}\alpha$	0.53–0.85	0.18–0.32	0.41–0.56	0.48–0.75	0.49–0.78
He II $\lambda 4686/\text{H}\beta$	< 0.14	~0.05	0.23–0.28	0.28–0.37	0.23–0.31
[Ne III] $\lambda 3869/\text{H}\beta$	0.37–0.92	0.18–0.21	0.50–0.72	0.71–1.1	1.2–1.6

NOTE.—The ranges predicted by the photoionizing shock models of DS95 and DS96 (shock + precursor)

VARIOUS LINE RATIOS OBSERVED IN NGC 5929 WITH THEIR CORRESPONDING VALUES OF A_{MII} FOR FOUR MB-IB
99Ferruit - Tabl.9 MODELS (MODEL S, B96; MODELS L, M AND H, B97)

Line Ratio	A_{MII} RANGES				
	Observed	Model S	Model L	Model M	Model H
[O III] $\lambda 5007/\text{H}\beta$	2.1–3.5	*	0.32–0.58	0.31–0.60	*
[O II] $\lambda 3727/\text{H}\beta$	3.4–5.1	2.3–0.94	< 0.62	1.5–0.49	1.3–0.16
[O I] $\lambda 6300/\text{H}\alpha$	0.30–0.52	*	< 0.39	< 0.30	< 0.74
[O II] $\lambda 3727/[\text{O III}]\lambda 5007$	1.0–2.0	0.43–0.22	0.57–0.28	0.74–0.35	< 0.18
[O I] $\lambda 6300/[\text{O III}]\lambda 5007$	0.39–0.77	*	0.35–0.17	0.34–0.15	*
[N II] $\lambda 6583/\text{H}\alpha$	0.42–0.75	4.0–1.4	3.8–0.78	4.6–1.3	4.2–1.4
[N II] $\lambda 6583/[\text{N I}]\lambda 5200$	3–16	*	< 101	< 143	< 1300
[S II] $\lambda \lambda 6717, 6731/\text{H}\alpha$	0.53–0.85	< 0.27	2.3–0.30	1.8–0.46	2.1–0.43
He II $\lambda 4686/\text{H}\beta$	< 0.14	< 0.32	< 0.57	< 0.53	< 0.66
[Ne III] $\lambda 3869/\text{H}\beta$	0.37–0.92	*	1.0–8.7	0.76–33	< 1.2

Results from our spectrophotometric study of NGC 5929

Date of observation: 19. 01.2012

Telescope and spectrograph: 1.93_m OHP telescope, CARELEC spectrograph

Spectroscopic data: 136 A/mm, $\lambda\lambda$ 3600 – 7200 A,
slit: width = 0.302 mm – corresponding to 2 arcsec on the sky
length = 50 mm - corresponding to 5.5 arcmin on the sky

Observer: prof. M. Dennefeld

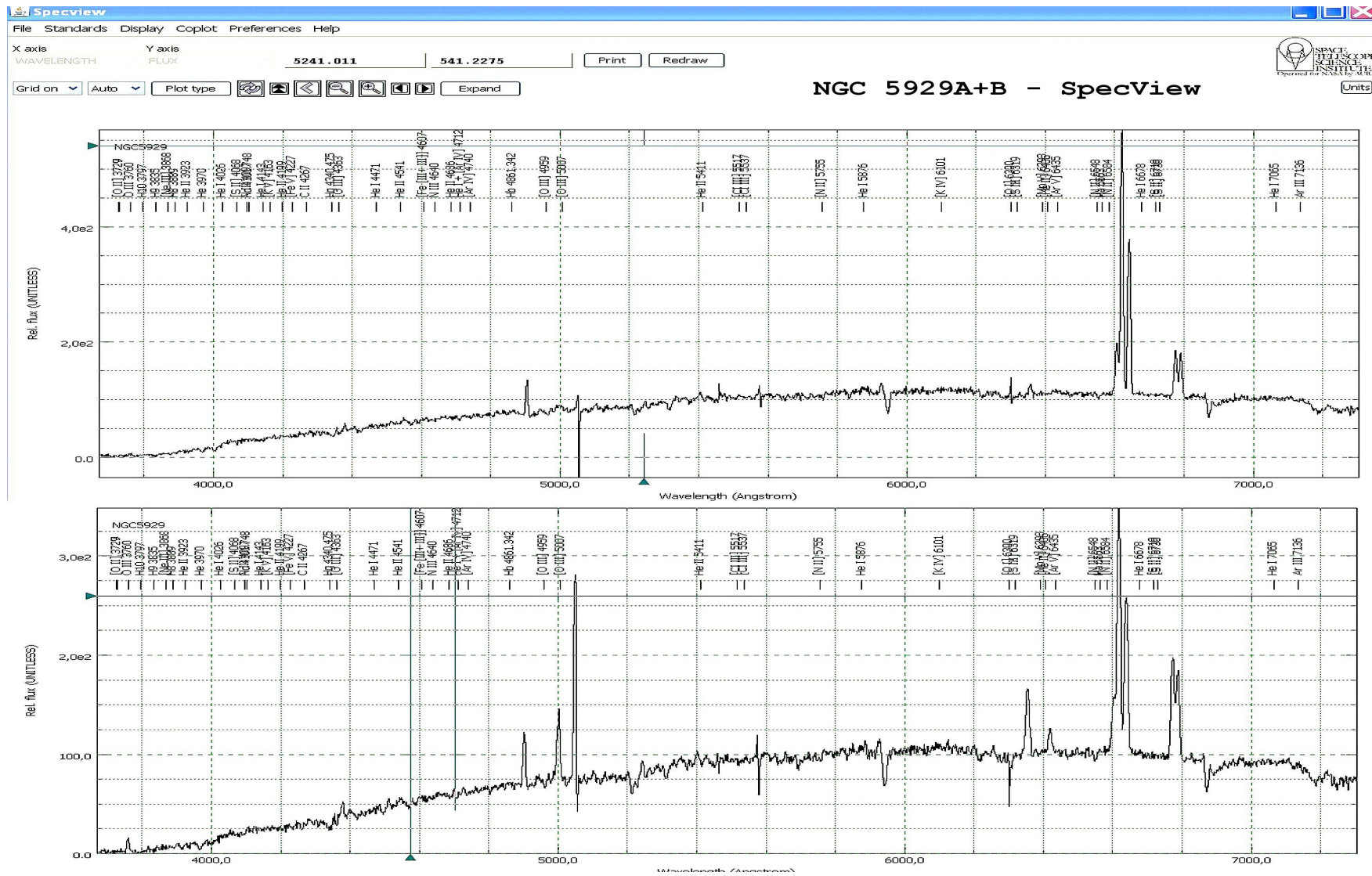
Time exposure: 1800 sec

Dev_type: CCD EEV 42-20

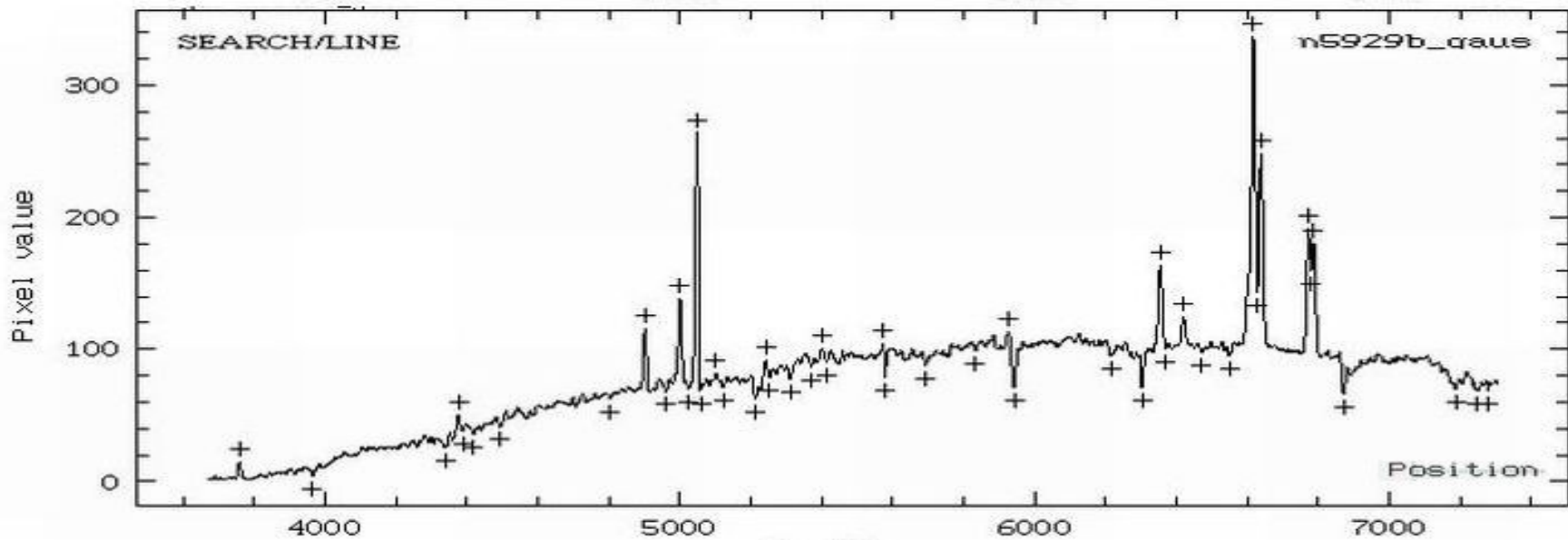
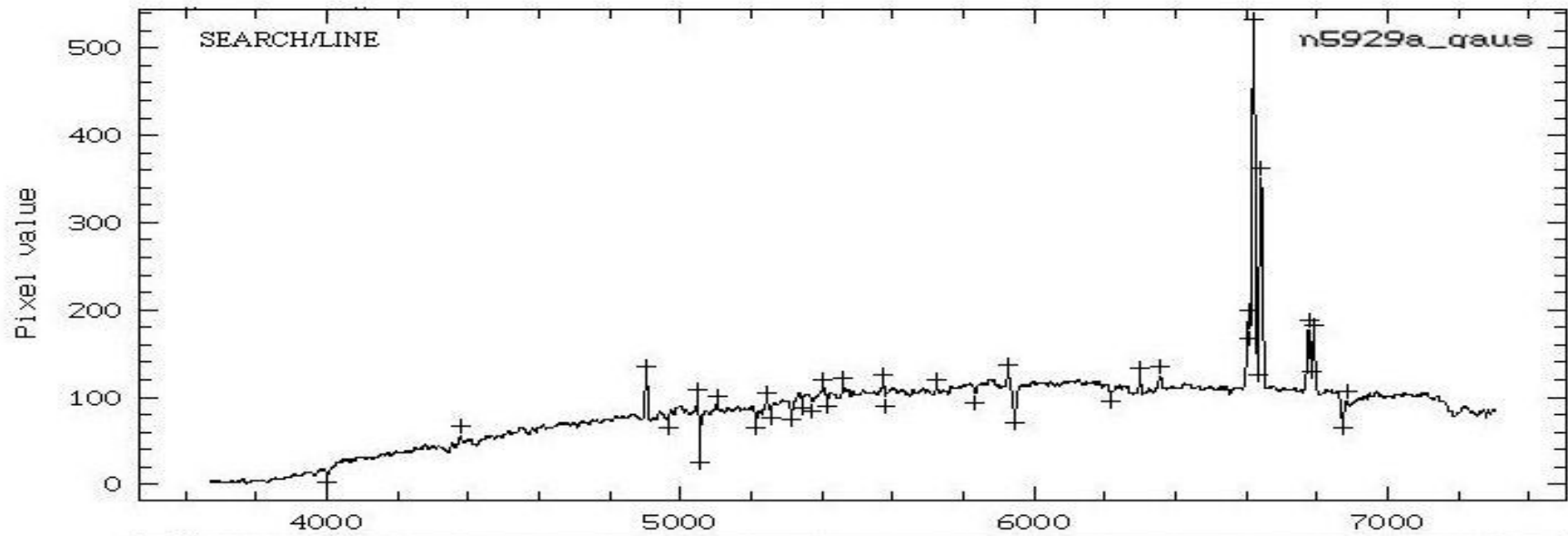
Objects: NGC 5929A = NE_lobe of NGC 5929
NGC 5929B = SW_lobe of NGC 5929

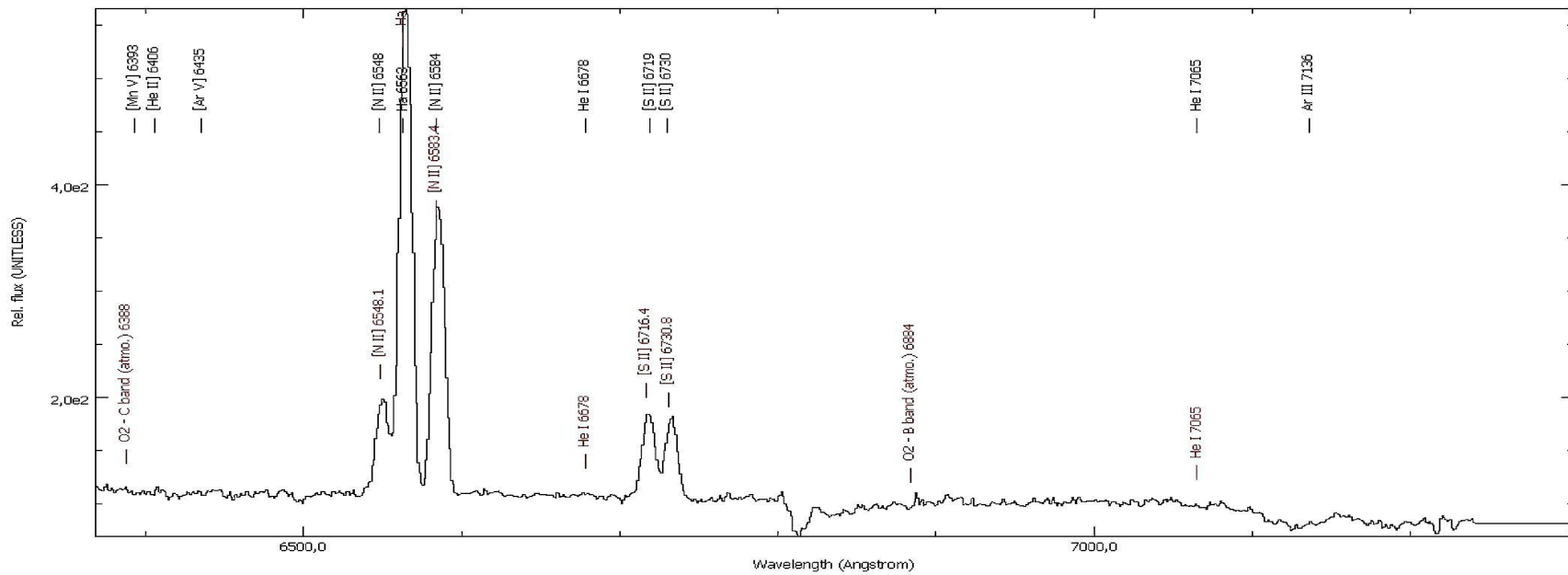
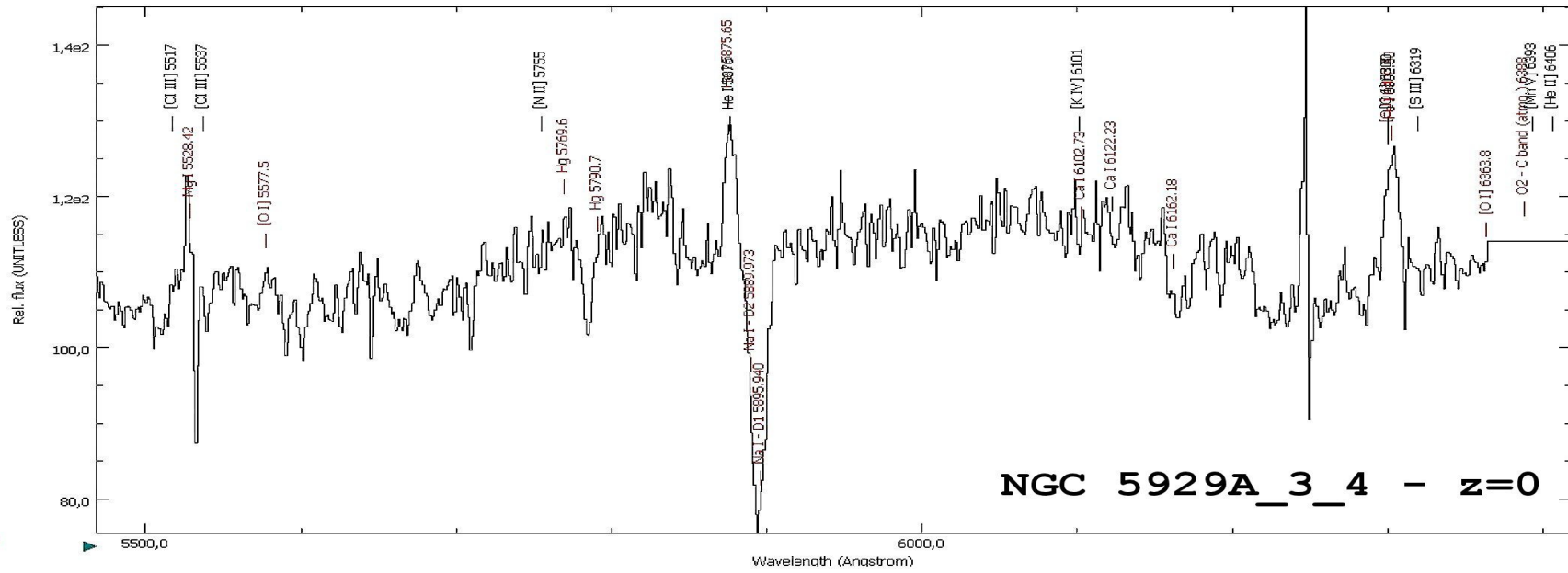
Observed line flux: in 10^{-14} ergs s⁻¹ cm⁻²

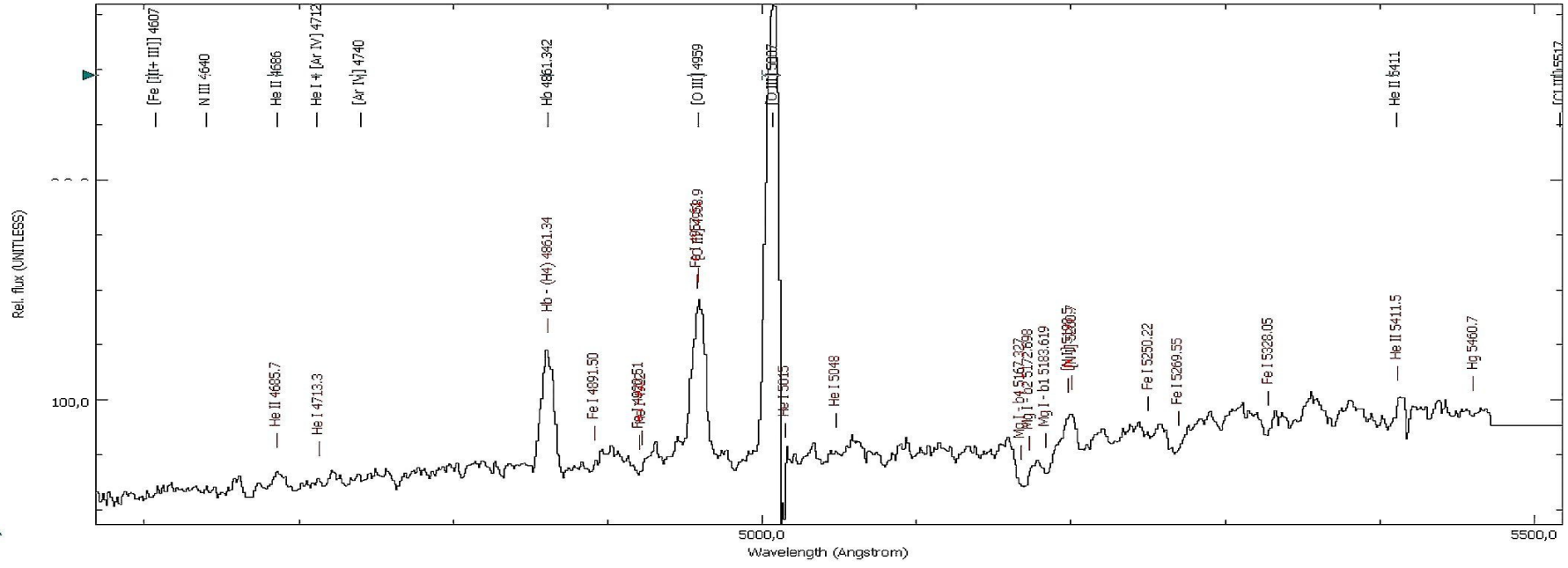
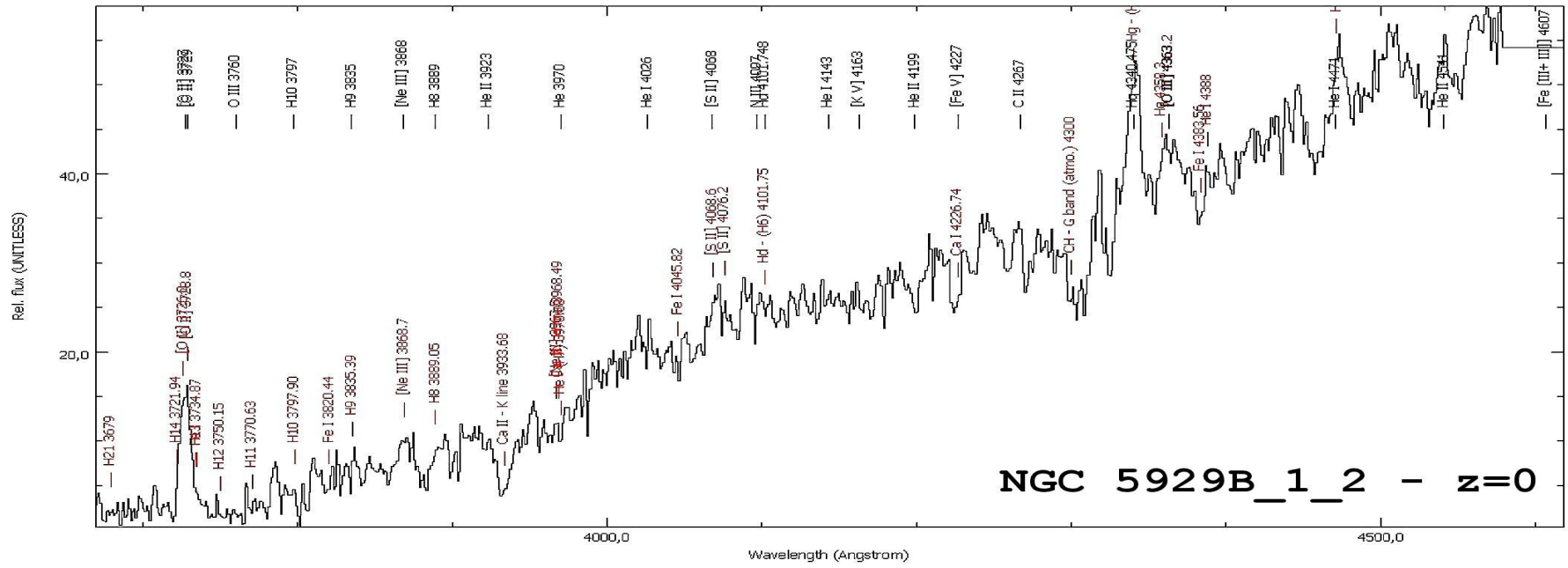
On the next slide the spectrograms of NGC 5929A and NGC 5929B together with typical emission lines for planetary and diffuse nebulae are presented:

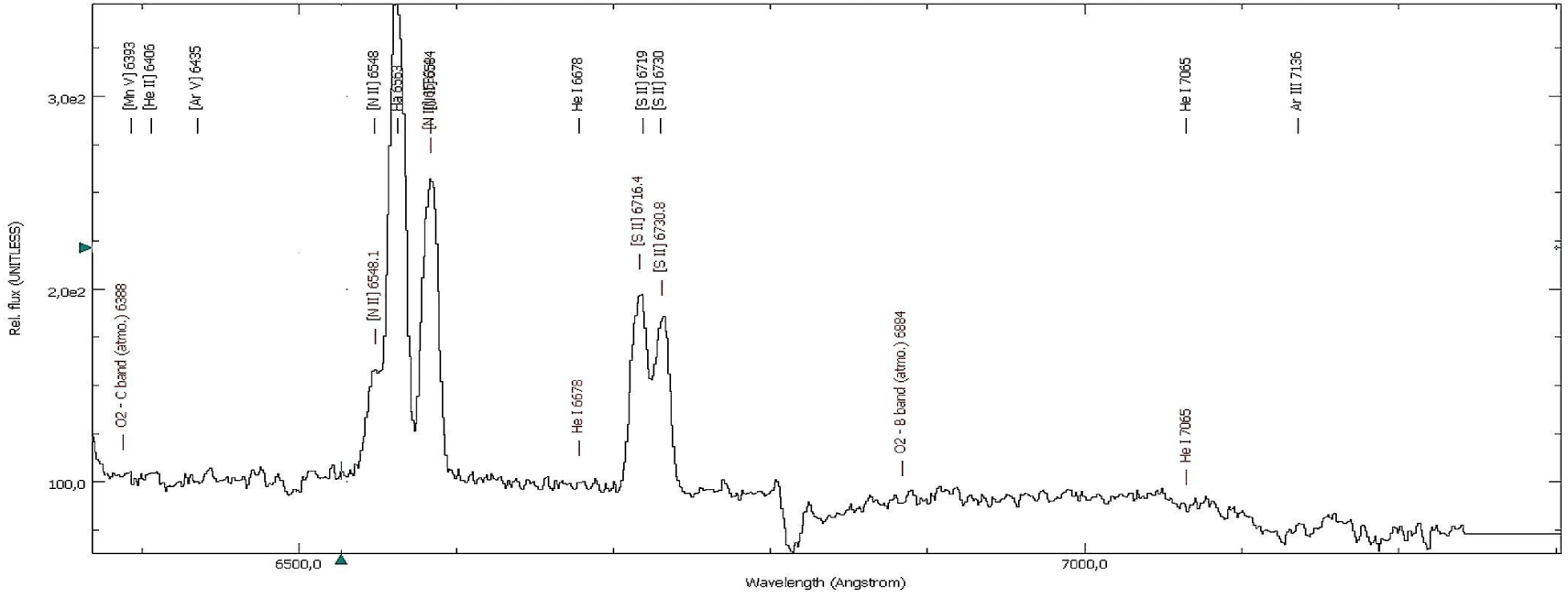
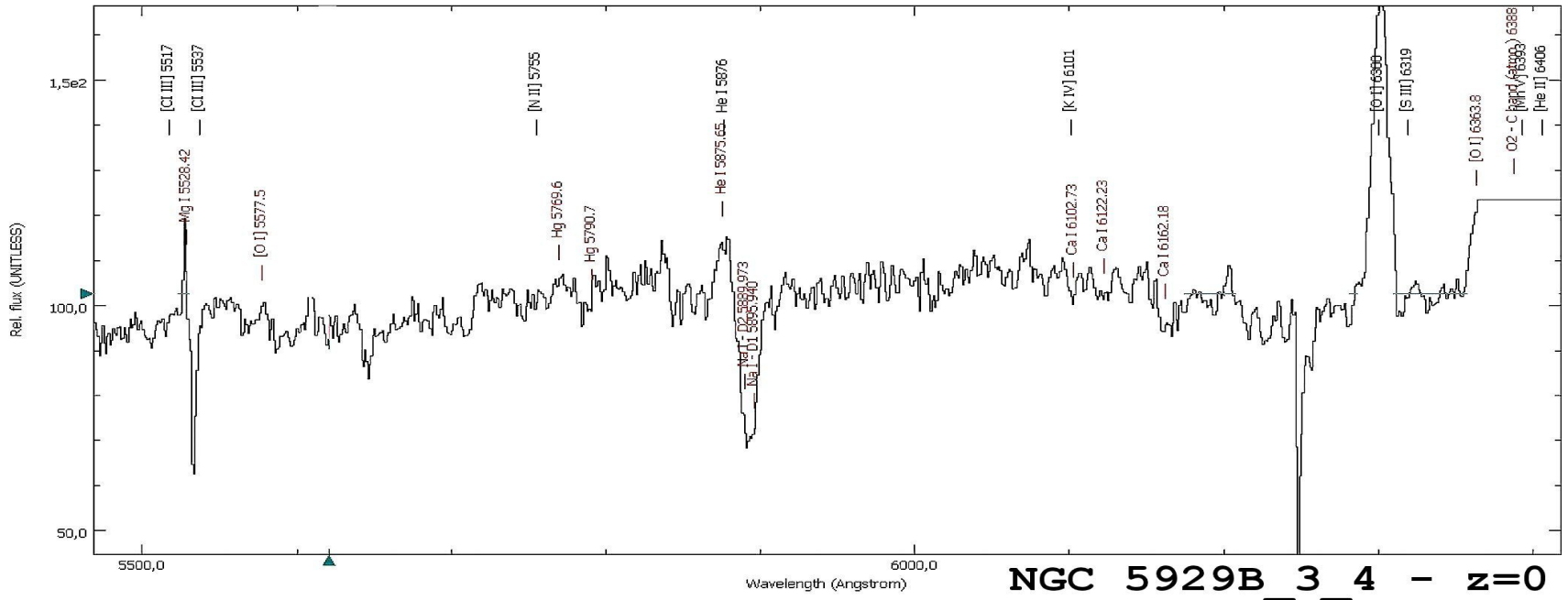


Results from MIDAS "SEARCH/LINE" procedure for absorption and emission lines ...









Results from MIDAS "INTEGRATE/LINE" procedure for NGC 5929A

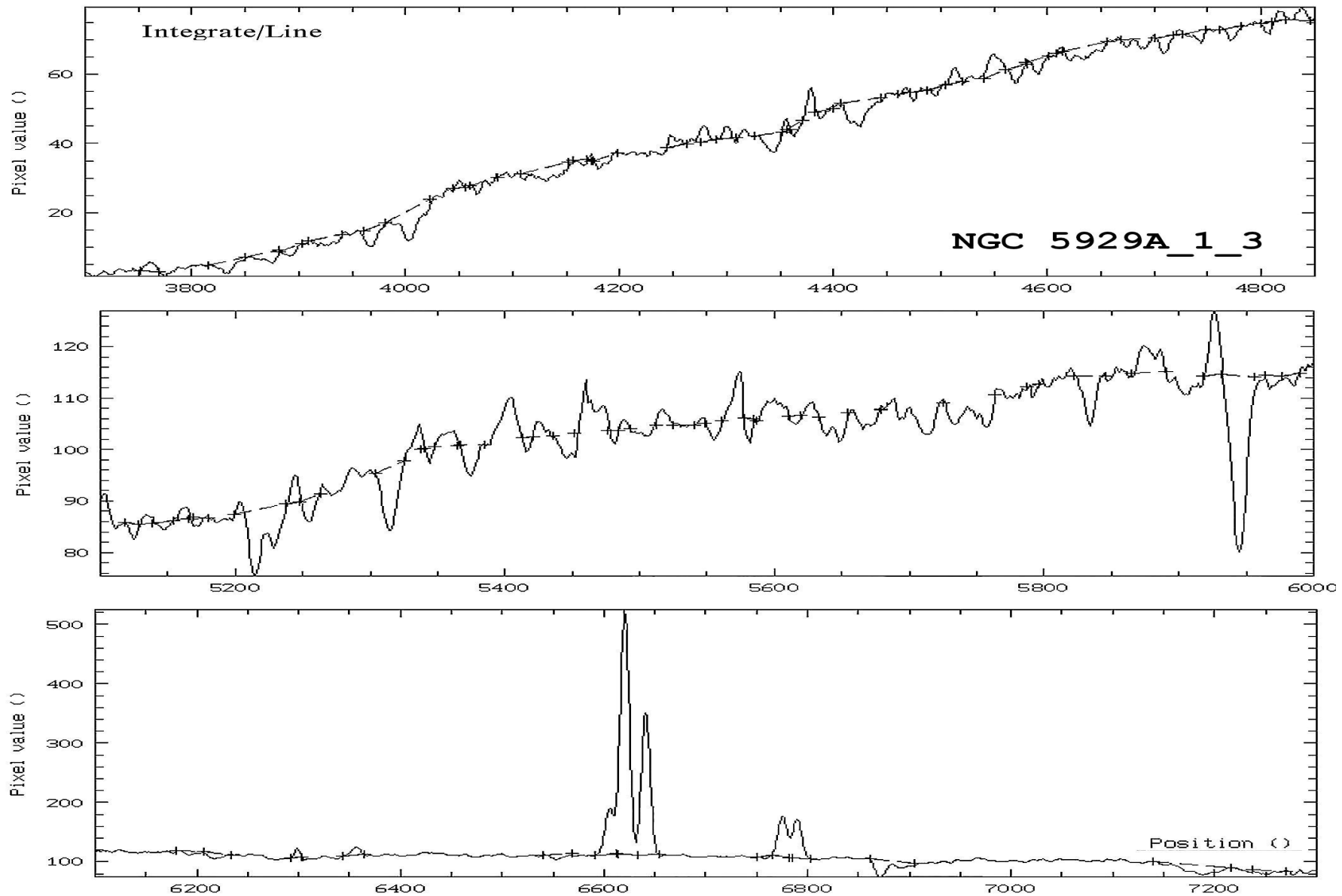


Table: n5929a_integr_line EQWT<0 = emission!!!

Seq	X_start	X_end	Flux	EQWT	X0	Ident	Bandpass
1	3753.00	3766.51	21.05	-6.26	3727.42	[OII]	
2	3849.76	3881.42	-50.72	6.27	3840.00	H9_blend	3822-3858
3	3960.59	3980.74	-65.78	4.15	3930.00	K_CaII	3908-3952
4	3983.91	4025.59	-160.59	7.78	3970.00	H_CaII	3952-3988
5	4318.45	4349.99	-94.47	2.18	4301.00	G_band	4284-4318
6	4370.27	4382.66	61.05	-1.29	4340.48	H_gamma	
7	4406.77	4444.19	-147.29	2.81	4386.06	Fe4383	4369-4420
8	4505.44	4517.83	26.24	-0.45	4471.60	HeI	
9	4560.77	4580.92	-42.52	0.68	4533.78	Fe4531	4514-4559
10	4576.40	4586.54	7.19	-0.12	4541.60	HeII	
11	4579.48	4601.07	-38.54	0.60	4552.00	Fe4531	4514-4559
12	4668.72	4717.66	-40.84	1.24	4658.24	C2-4668	4634-4720
13	4716.08	4734.10	22.69	-0.32	4685.70	HeII	
14	4734.10	4748.74	-21.07	0.29	4698.23	C2-4668	4634-4720
15	4894.05	4909.82	403.47	-5.28	4861.34	H_beta	
16	4909.82	4923.34	-27.66	0.36	4871.98	Hbeta	4847-4876
17	4967.27	4978.53	34.45	-0.43	4931.00	[OIII]	
18	5010.07	5020.21	14.47	-0.18	4972.10	[FeVI]	
19	5021.33	5092.30	-23.06	3.56	5012.79	Fe5015	4977-5054
20	5113.70	5180.03	-28.91	0.52	5105.27	Mg1	5069-5134

21	5198.18	5207.19	15.80	-0.18	5158.98	[FeVII]	
22	5199.18	5237.48	-198.57	2.25	5168.29	Mg2	5154-5196
23	5237.60	5248.87	35.28	-0.39	5199.00	[NI]	
24	5303.94	5325.34	-144.90	1.50	5268.18	Fe5270	5245-5285
25	5367.14	5385.16	-48.00	0.48	5330.89	Fe5335	5312-5352
26	5433.60	5455.00	-86.55	0.83	5398.30	Fe5406	5387-5415
27	5455.00	5466.26	56.16	-0.54	5410.80	HeII	
28	5466.26	5476.40	29.26	-0.28	5423.90	[FeVI]	
29	5560.88	5575.53	68.35	-0.65	5517.66	[ClIII]	
30	5676.90	5691.55	19.44	-0.18	5630.82	[FeVI]	
31	5727.59	5762.51	-102.62	0.94	5699.24	Fe5709	5696-5720
32	5821.08	5842.48	-102.07	0.89	5784.96	Fe5782	5776-5796
33	5822.08	5845.74	-87.50	0.77	5790.70	Hg	
34	5919.08	5933.72	114.32	-1.01	5875.65	HeI	
35	5931.35	5956.13	-434.47	3.80	5893.03	NaD	5876-5909
36	6028.34	6046.36	-22.87	0.20	5983.01	TiO1	5936-5994
37	6255.88	6293.05	-124.97	1.14	6216.58	TiO2	6189-6272
38	6341.48	6368.52	145.08	-1.32	6300.00	[OI]	
39	6591.19	6613.72	1099.54	-9.83	6548.88	[NII]	
40	6612.22	6633.24	4387.74	-38.96	6562.81	H_alpha	
41	6633.24	6654.27	2494.67	-22.30	6583.83	[NII]	
42	6765.41	6784.93	807.25	-7.42	6716.42	[SII]	
43	6781.93	6802.95	730.68	-6.91	6730.78	[SII]	

Results from MIDAS "INTEGRATE/LINE" procedure for NGC 5929B

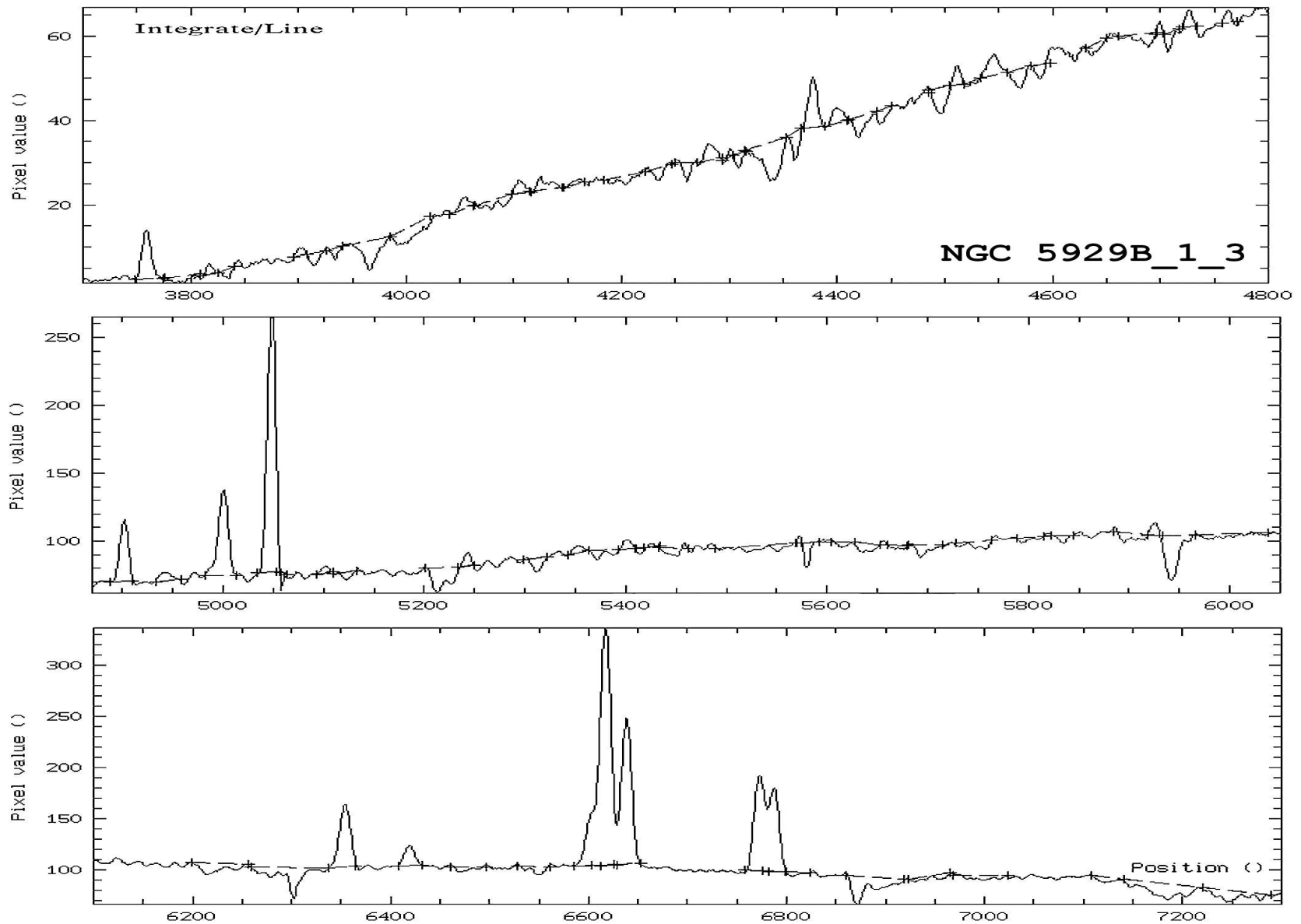
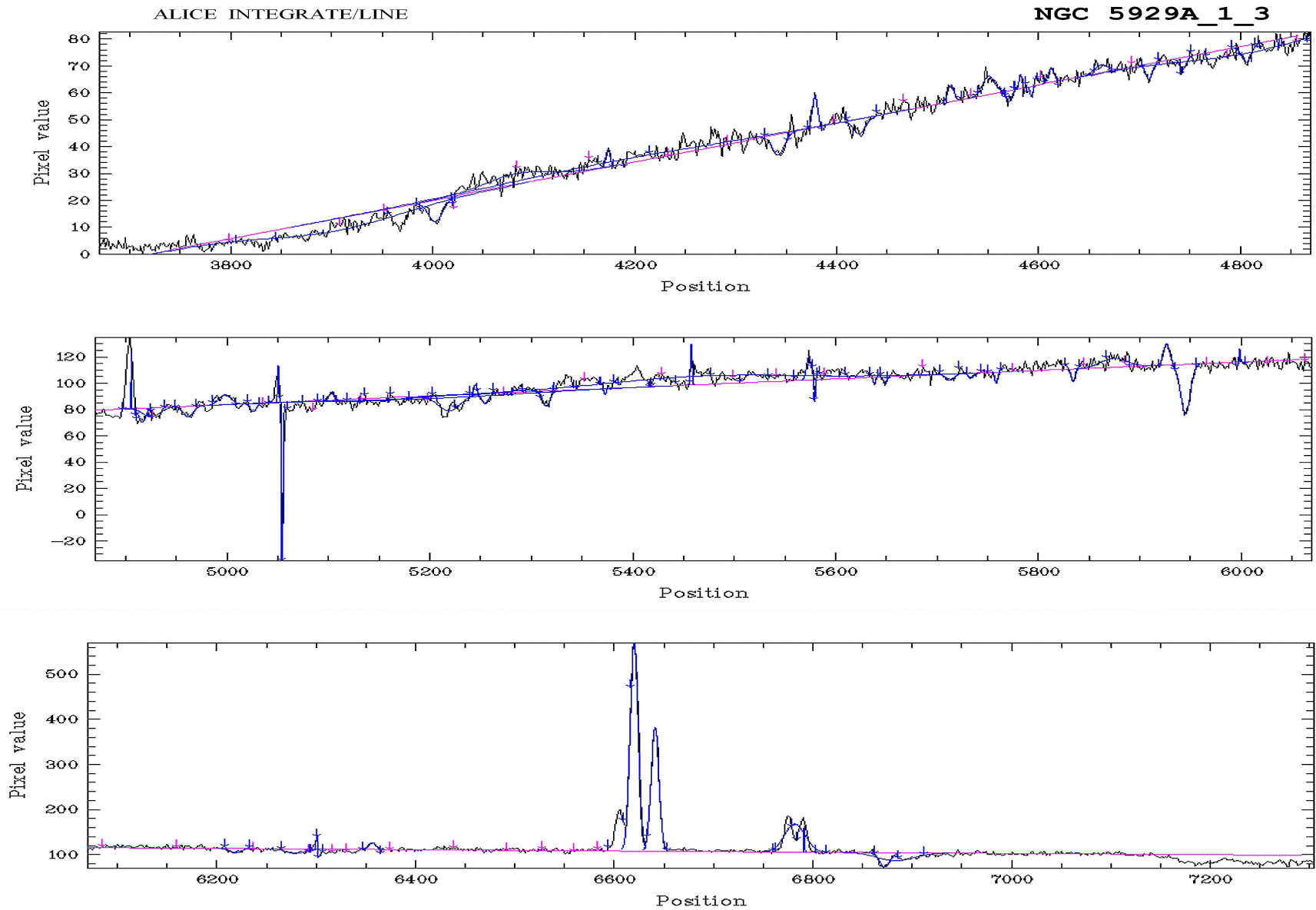


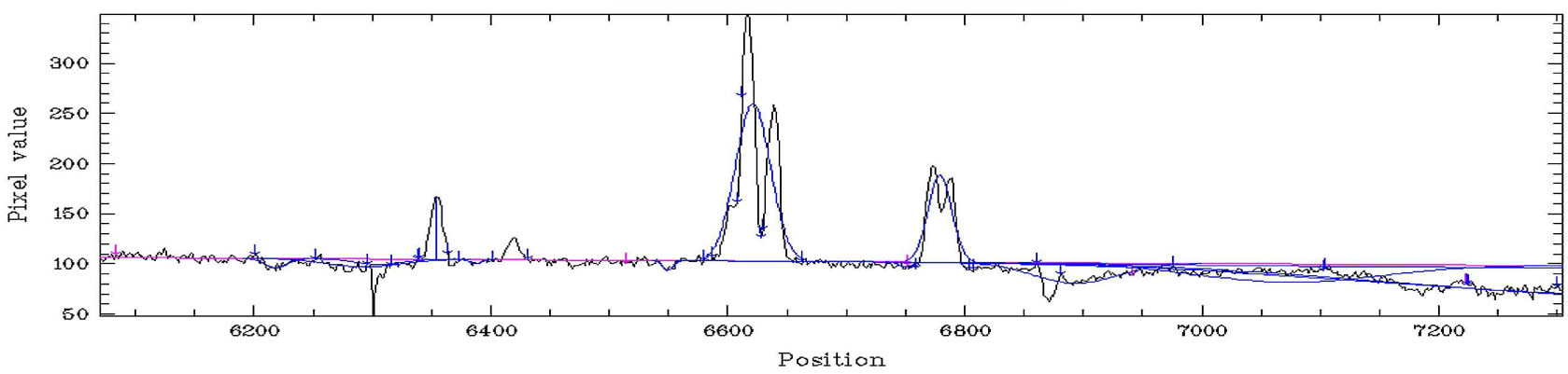
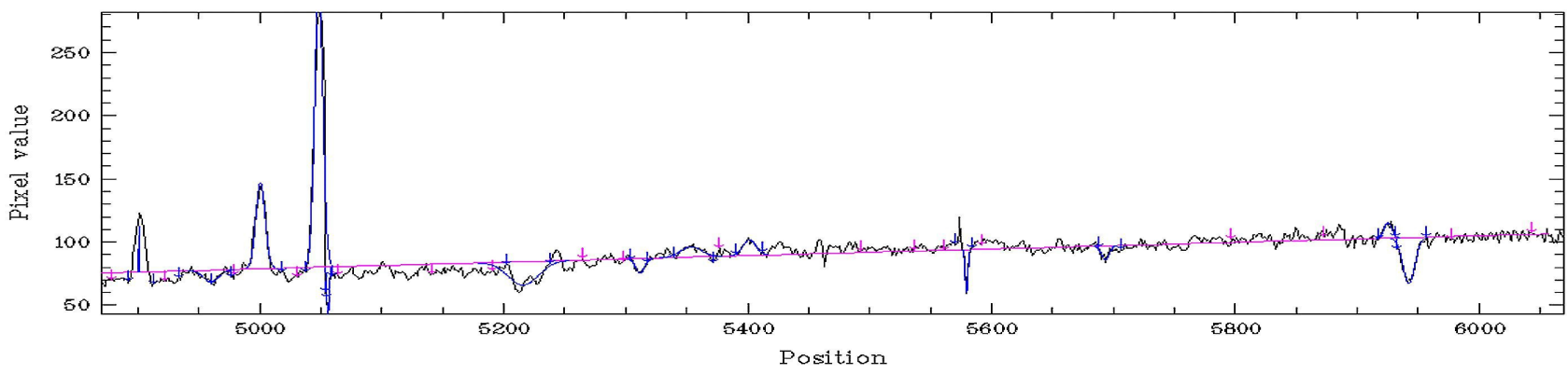
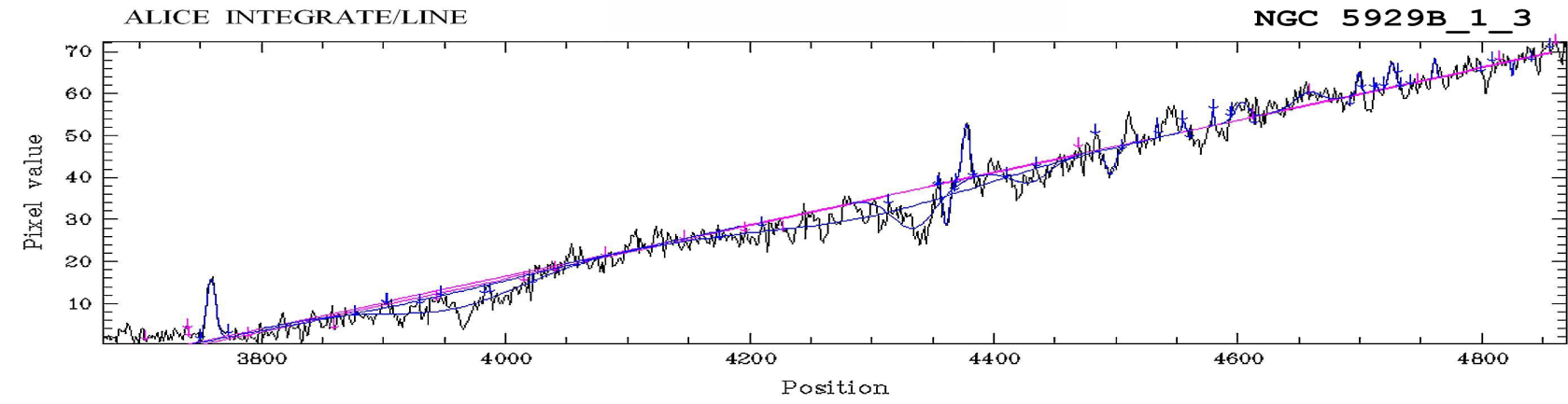
Table: n5929b_integr_line_ident EQWT<0 = emission!!!

Seq	X_start	X_end	Flux	EQWT	X0_2	Ident	Bandpass
1	3749.62	3772.15	106.33	-38.02	3727.42	[OII]	
2	3893.80	3908.44	18.47	-2.43	3868.76	[NeIII]	
3	3907.95	3925.85	-25.70	2.94	3889.00	HeI&H8	
4	3954.62	3979.41	-67.71	6.50	3930.00	K_CaII	3908-3952
5	3987.29	4023.34	-55.17	3.91	3970.00	H_CaII	3952-3988
6	4097.94	4115.84	28.52	-1.25	4068.60	[SII]	
7	4249.38	4270.03	-25.89	0.86	4225.44	Ca4227	4222-4234
8	4314.09	4352.63	-177.25	5.15	4301.00	G_band	4284-4318
9	4369.16	4388.43	109.85	-2.86	4340.48	H_gamma	
10	4389.42	4410.82	37.76	-0.96	4368.74	[OIII]+?	Blend?
11	4410.82	4429.97	-48.37	1.18	4386.06	Fe4383	4369-4420
12	4504.31	4516.70	23.78	-0.49	4471.60	HeI	
13	4557.77	4597.69	-49.10	1.29	4539.94	Fe4531	4514-4559
14	4700.31	4718.33	-43.48	0.70	4668.62	C2-4668	4634-4720
15	4720.22	4733.99	25.24	-0.41	4685.70	HeII	
16	4887.80	4909.95	456.73	-6.50	4861.34	H_beta	
17	4930.09	4952.62	65.58	-0.92	4893.40	[FeVII]	
18	4952.62	4966.14	-37.29	0.51	4924.00	FeII	
19	4966.14	4979.66	12.64	-0.17	4931.00	[OIII]	
20	4982.31	5013.33	753.70	-10.09	4958.90	[OIII]	

21	5034.85	5056.25	1820.00	-23.50	5006.80	[OIII]	
22	5057.63	5091.54	-28.75	0.76	5027.85	Fe5015	4977-5054
23	5113.70	5174.52	-57.63	1.07	5102.90	Mg1	5069-5134
24	5198.18	5234.22	-306.15	3.85	5168.29	Mg2	5154-5196
25	5234.22	5247.74	78.06	-0.96	5199.00	[NI]	
26	5301.81	5331.10	-126.41	1.42	5268.18	Fe5270	5245-5285
27	5363.34	5392.88	-93.23	1.00	5330.89	Fe5335	5312-5352
28	5566.51	5575.53	27.19	-0.28	5517.66	[ClIII]	
29	5728.12	5763.57	-112.99	1.13	5699.24	Fe5709	5696-5720
30	5824.46	5840.23	-45.76	0.44	5784.96	Fe5782	5776-5796
31	5822.64	5844.79	-46.96	0.45	5790.70	Hg	
32	5918.63	5933.40	65.61	-0.63	5875.65	HeI	
33	5930.34	5963.01	-471.42	4.54	5893.03	NaD	5876-5909
34	5965.89	6038.26	-107.41	1.02	5956.38	TiO1	5936-5994
35	6259.27	6337.37	-591.21	5.79	6240.40	TiO2	6189-6272
36	6340.36	6367.39	783.29	-7.62	6300.00	[OI]	
37	6407.96	6431.99	239.90	-2.31	6363.80	[OI]+?	
38	6407.94	6433.85	227.61	-2.18	6374.00	[FeX]	
39	6585.18	6612.22	1134.14	-10.96	6548.88	[NII]	
40	6587.04	6609.57	754.41	-7.20	6548.88	[NII]	
41	6603.20	6628.74	3308.84	-31.70	6562.81	H_alpha	
42	6625.73	6652.77	1928.58	-18.24	6583.83	[NII]	
43	6757.90	6781.93	1286.89	-13.01	6716.42	[SII]	
44	6775.92	6799.95	1290.31	-13.10	6730.78	[SII]	

Results from MIDAS "ALICE - INTEGRATE/LINE" procedure for NGC 5929A and B





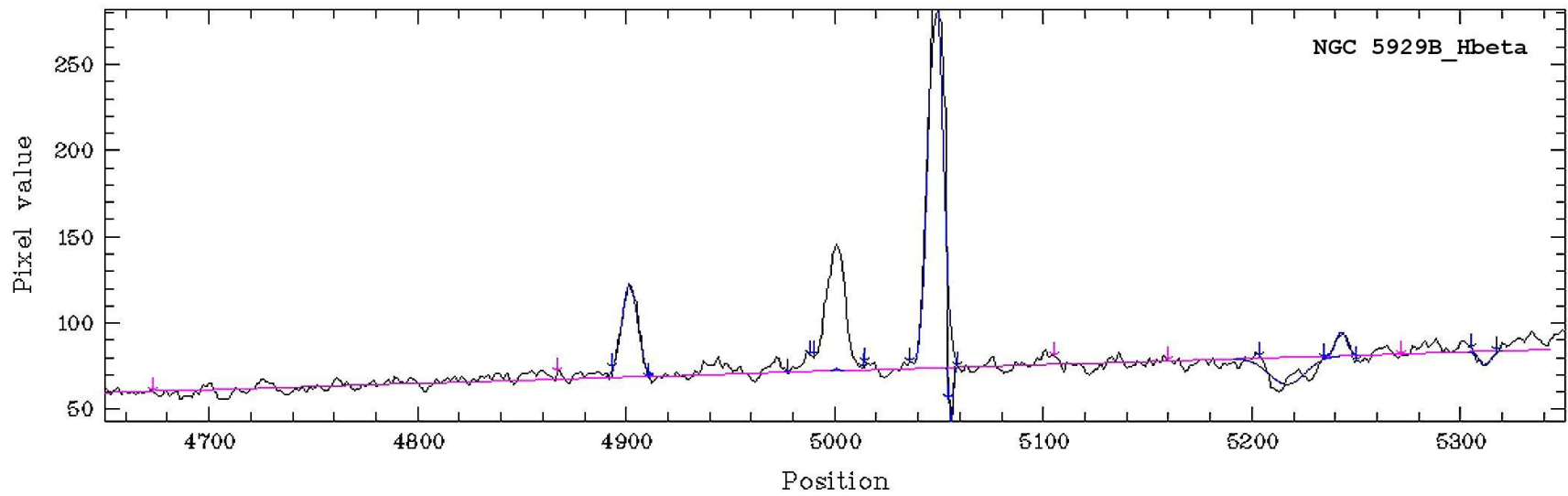
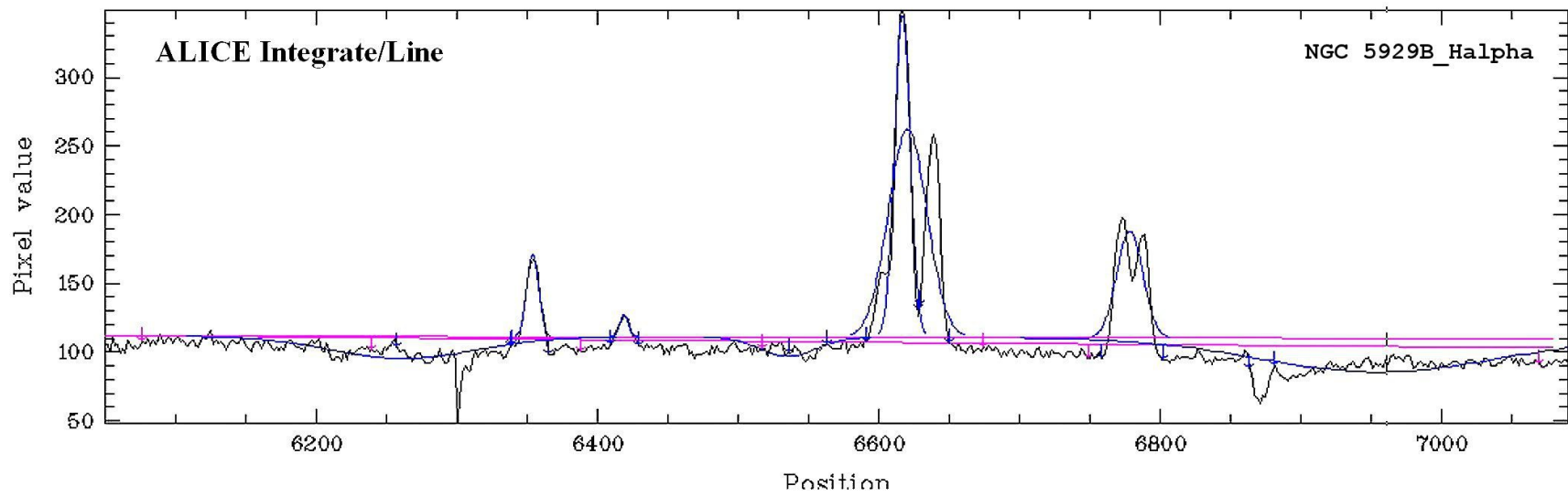


Table: n5929b_hbs&has_integr_ident EQWT<0 = emission!!!

Seq	X_start	X_end	Flux	EQWT	X0	Ident
1	4891.64	4910.66	475.52	-6.86	4861.342	H_beta
2	4981.75	5011.79	728.48	-9.66	4958.930	[O III]
3	5035.82	5055.84	1864.99	-24.83	5006.860	[O III]
4	5055.84	5059.85	-17.16	0.23	5015.000	abs?
5	6334.10	6366.01	842.86	-8.37	6300.310	[O I]
6	6407.94	64.33.85	227.61	-2.18	6374.00	[FeX]
7	6406.44	6429.84	238.95	-2.30	6363.800	[O I]
8	6586.22	6610.69	857.72	-8.11	6548.060	[N II]
9	6604.31	6630.90	3315.86	-31.35	6562.808	H_alpha
10	6625.58	6653.24	1961.66	-18.71	6583.370	[N II]
11	6759.63	6783.03	1401.31	-14.43	6716.420	[S II]
12	6776.65	6798.99	1241.31	-12.66	6730.780	[S II]

NGC5929A&B_integr_line_emiss: NGC 5929A

NGC 5929B

Seq	X0	Ident	Flux	EQWT	F/F_H β	Flux	EQWT	F/F_H β
1	3727.42	[OII]	21.05	-6.26	0.052	106.33	-38.02	0.233
2	3868.76	[NeIII]	18.47	-2.43	0.040
3	4068.60	[SII]	28.52	-1.25	0.062
4	4340.48	H_gamma	61.05	-1.29	0.15	109.85	-2.86	0.240
5	4368.74	[OIII]+?	37.76	-0.96	0.083
6	4471.60	HeI	26.24	-0.45	0.065	23.78	-0.49	0.052
7	4541.60	HeII	7.19	-0.12	0.018
8	4685.70	HeII	22.69	-0.32	0.056	25.24	-0.41	0.055
9	4861.34	H_beta	403.47	-5.28	1.00	456.73	-6.50	1.00
10	4893.40	[FeVII]	65.58	-0.92	0.144
11	4931.00	[OIII]	34.45	-0.43	0.085	12.64	-0.17	0.028
12	4958.90	[OIII]	753.70	-10.09	1.650
13	4972.10	[FeVI]	14.47	-0.18	0.036
14	5006.80	[OIII]	1820.00	-23.50	3.985
15	5158.98	[FeVII]	15.80	-0.18	0.039
16	5199.00	[NI]	35.28	-0.39	0.087	78.06	-0.96	0.171
17	5410.80	HeII	56.16	-0.54	0.139	27.19	-0.28	0.060
18	5423.90	[FeVI]	29.26	-0.28	0.072
19	5517.66	[ClIII]	68.35	-0.65	0.169	65.61	-0.63	0.144
20	5630.82	[FeVI]	19.44	-0.18	0.048	783.29	-7.62	1.715
21	5875.65	HeI	114.32	-1.01	0.283	239.90	-2.31	0.525
22	6300.00	[OI]	145.08	-1.32	0.360	227.61	-2.18	0.498
23	6363.80	[OI]+?	1134.14	-10.96	2.483
24	6374.00	[FeX]	227.61	-2.18	0.498
25	6548.88	[NII]	1099.54	-9.83	2.725	754.41	-7.20	1.652
26	6562.81	H_alpha	4387.74	-38.96	10.875	3308.84	-31.70	7.245
27	6583.83	[NII]	2494.67	-22.30	6.183	1928.58	-18.24	4.222
28	6716.42	[SII]	807.25	-7.42	2.001	1286.89	-13.01	2.818
29	6730.78	[SII]	730.68	-6.91	1.811	1290.31	-13.10	2.825

Flux ratios for NGC 5929 and predictions of some models				
	NGC 5929A	NGC 5929B	models	
Rad. Velocities [km/sec]	2595	2526	Vs = 300 km/s	L_model
Ratio				
[OIII] 5007 / Hbeta		3.956	5.9 – 6.5	0.32 – 0.58
[OII] 3727 / Hbeta	0.017	0.232	1.7 – 5.2	< 0.62
[OI] 6300 / Halpha	0.033	0.254	0.32 – 0.47	< 0.39
[OII] 3727 / [OIII] 5007		0.058	0.3 – 0.8	0.57 – 0.28
[OI] 6300 / [OIII] 5007		0.300	0.15 – 0.23	0.35 – 0.17
[OIII] 5007 / [OIII] 4363		48.20	103 - 108	3.8 – 0.78
[NII] 6583 / Halpha	0.568	0.590	0.23 – 0.65	< 101
[SII] 6724 / Halpha	0.350	0.785	0.41 – 0.56	2.3 – 0.30
[He II] 4686 / Hbeta	0.056	0.055	0.23 – 0.28	< 0.57
[NeIII] 3869 / Hbeta		0.040	0.50 – 0.72	1.0 – 8.7
[SII] 6717 / [SII] 6731	1.105	1.129		
[OIII] 4959+5007 / [OIII] 4363		68.16		
Ne for Te = 10 000 K	470	450		

Abundances of some ions for $T_e = 10\,000\text{K}$;		Log H = 12.00	
		NGC 5929A	NGC 5929B
Log N⁺	(λ 6584/Hbeta)	7.99	7.83
Log S⁺	(λ (6717+6731)/Hbeta)	7.22	7.39
Log O⁺⁺	(λ 5007/Hbeta)	-	8.10
Log O⁺	(λ 3727/Hbeta)	5.96	7.00
Log O[°]	(λ 6300/Hbeta)	7.70	7.84
Log He⁺	(λ 5876/Hbeta)	11.32	11.59
Log He⁺⁺	(λ 4685/Hbeta)	9.75	9.74

Thank You!